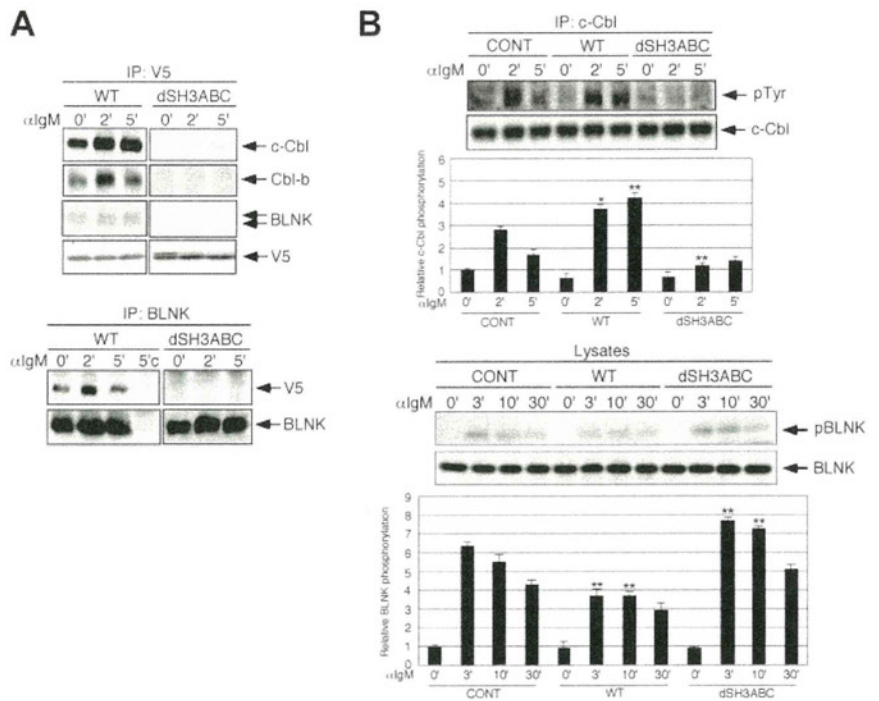


Figure 1. CIN85 associates with Cbl and BLNK and regulates their phosphorylation in B cells. (A) BJAB cells stably expressing either WT or SH3-deleted CIN85 were stimulated with 20 $\mu\text{g}/\text{mL}$ of $\text{F}(\text{ab}')_2$ goat anti-human IgM for the indicated time periods. Immunoprecipitates with anti-V5 or anti-BLNK mAb were separated on a 10% SDS-PAGE gel and analyzed by Western blotting with anti-c-Cbl, anti-Cbl-b, or anti-V5 mAb. 5'c, immunoprecipitation of the cell lysates at 5 minutes with isotype control. (B) Control BJAB cells and stable transformants expressing either WT or SH3-deleted CIN85 were stimulated with 20 $\mu\text{g}/\text{mL}$ of $\text{F}(\text{ab}')_2$ goat anti-human IgM for the indicated time periods. Immunoprecipitates with anti-c-Cbl mAb were separated on a 10% SDS-PAGE gel and analyzed by Western blotting with anti-phosphotyrosine or anti-c-Cbl mAb. The resulting values are expressed as fold changes in protein expression compared with unstimulated control cells. The values are the mean \pm SD of 3 independent experiments (* $P < .05$, ** $P < .01$ vs controls). (C) Control BJAB cells and stable transformants expressing either WT or SH3-deleted CIN85 were stimulated with 20 $\mu\text{g}/\text{mL}$ of $\text{F}(\text{ab}')_2$ goat anti-human IgM for the indicated time periods. The cell lysates were subsequently separated on a 10% SDS-PAGE gel and analyzed by Western blotting with anti-phospho-BLNK or anti-BLNK mAb. The resulting values are expressed as fold changes in protein expression compared with unstimulated control cells. The values are the mean \pm SD of 3 independent experiments (** $P < .01$ vs controls).



and immediately measuring the luminescence on a Lumat LB9507 luminometer (EG & G Berthold). To serve as a control for the transfection efficiency, the relative luciferase activity of the medium and cells stimulated with BCR was calculated relative to stimulation with PMA/ionomycin.

Flow cytometric analysis

BJAB cells were incubated on ice for 15 minutes with 20 $\mu\text{g}/\text{mL}$ goat-unlabeled anti-IgM before they were washed with ice-cold medium and warmed at 37°C for the indicated time intervals. The cells were washed with ice-cold PBS containing 2% FBS and 0.2% sodium azide (Fisher Scientific) to stop internalization at the assigned time points and to remove the unbound Ab. The remaining surface BCRs were stained with FITC-labeled rabbit anti-goat Ig and quantified by flow cytometry. The data are presented as the percentage of surface BCR remaining.

Fluorescence microscopic analysis

BJAB cells were incubated with 10 $\mu\text{g}/\text{mL}$ of unlabeled goat anti-human IgM sera (20 $\mu\text{g}/\text{mL}$) at 4°C for 30 minutes and warmed to 37°C for the indicated time periods. The cells were then fixed with 3.7% paraformaldehyde and permeabilized with PBS containing 1% BSA and 0.05% saponin (wash buffer). The cells were then incubated for 30 minutes with FITC-conjugated anti-goat IgG pAb (Jackson ImmunoResearch Laboratories) at 4°C. The stained cells were centrifuged onto slides and analyzed with inverted fluorescent microscopy (BZ-9000; Keyence).

Quantitative real-time PCR

The total RNA was extracted from the primary B cells using Isogen reagent (Nippon gene) and was treated with DNase I (Invitrogen) to remove contaminating genomic DNA. First-strand cDNA was synthesized using a QuantiTect reverse transcription kit (QIAGEN). Quantitative real-time PCR was performed in the ABI Prism 7700 Sequence Detector (Applied Biosystems). The reactions were performed in triplicate wells in 96-well plates. TaqMan target mixes for Cyclin D2, Myc, *BCL2L1/BclxL*, *BCL2A1/A1*, *PRDM1/Blimp-1*, and *XBP1* were purchased from Applied Biosystems. 18S ribosomal RNA (rRNA) was separately amplified in the same plate as an internal control for variation in the amount of cDNA in PCR. The collected data were analyzed using the Sequence Detector software

(Applied Biosystems). The data were expressed as the fold change in gene expression relative to the expression in the control cells.

Annexin V staining

After culture, cells ($1-2 \times 10^5$) were washed twice with PBS and suspended in 85 μL binding buffer (MBL) containing Ca^{2+} . The cell suspension supplemented with 10 μL annexin-V-FITC or annexin-V-PE (MBL) and 5 μg of propidium iodide (PI) or 1 μg of 7-ADD was incubated at room temperature for 15 minutes in the dark. Subsequently, binding buffer was added, and the fraction of early apoptotic cells was measured using flow cytometry.

BrdU assay

DNA synthesis was monitored by pulse-labeling cells for 2 hours with the thymidine analog 5-bromo-2'-deoxyuridine (BrdU). The cells were washed 3 times with PBS and fixed for 20 minutes at -20°C in an ethanol fixative (0.15M glycine in 70% EtOH, pH 2.0). After rehydration in PBS, BrdU incorporation was detected by incubation with an anti-BrdU mAb for 1 hour at 37°C, followed by a rhodamine-conjugated anti-mouse antibody (1:500; Jackson ImmunoResearch Laboratories) and staining of the nucleus with 4'-6-diamidino-2-phenylindole for 1 hour. The proportion of BrdU-positive nuclei (BrdU labeling index) was assessed, based on a sample size of 500 cells per data point.

Statistical analysis

Statistical analysis was performed using the Student *t* test. $P < .05$ was considered statistically significant.

Results

CIN85 associates with Cbl and BLNK and regulates their phosphorylation

The tyrosine phosphorylation of signaling molecules is a critical event in BCR signaling.^{1,2} Because SH3 domains play an important role in the function of CIN85,²⁵ we focused on

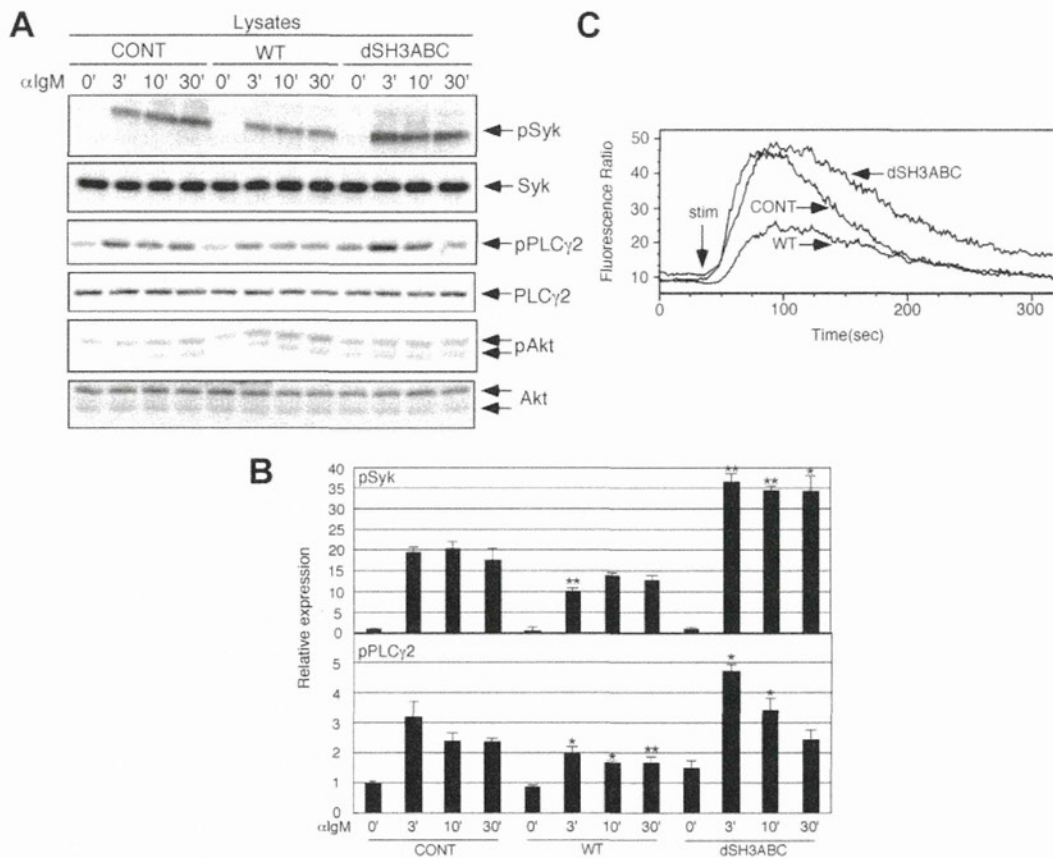


Figure 2. Forced CIN85 expression inhibits BCR-induced calcium flux and phosphorylation of Syk and PLCγ2. (A-B) Control BJAB cells and stable transformants expressing either WT or SH3-deleted CIN85 were stimulated with 20 μg/mL of F(ab')₂ goat anti-human IgM for the indicated time periods. The cell lysates were subsequently separated on a 10% SDS-PAGE gel and analyzed by Western blotting with anti-phospho-Syk pAb, anti-Syk mAb, anti-phospho-PLCγ2 pAb, anti-PLCγ2 pAb, anti-phospho-Akt pAb, or anti-Akt pAb. The resulting values are expressed as fold changes in protein expression compared with unstimulated control cells. The values are the mean ± SD of 3 independent experiments (**P* < .05, ***P* < .01 vs controls). (C) Ca²⁺ influx in control BJAB cells and stable transformants expressing either WT or SH3-deleted CIN85. The intracellular free calcium levels in Fluo 4/AM-loaded cells were analyzed using flow cytometry after the cells were stimulated with 20 μg/mL F(ab')₂ goat anti-human IgM. The results shown are representative of 4 independent experiments.

tyrosine-phosphorylated molecules downstream of the BCR that could associate with the SH3 domains of CIN85. Specifically, we focused on the 2 molecules, BLNK and c-Cbl, that function as key positive and negative regulators of BCR signaling,^{1,10} respectively; both proteins can associate with the SH3 domains of CIN85.^{14,26}

We first determined the association of Cbl and BLNK with CIN85 using WT and SH3-deleted CIN85-expressing B cell lines. Consistent with previous reports,^{14,26} WT CIN85 was constitutively associated with c-Cbl and BLNK, and these associations were increased after BCR stimulation (Figure 1A). Cbl-b was similarly associated with WT CIN85, albeit to a lesser extent. Although the association of WT CIN85 and BLNK appeared modest, the inverse immunoprecipitation of BLNK confirmed the association (Figure 1A). As expected, the association of Cbl and BLNK with CIN85 was abrogated in SH3-deleted CIN85-expressing B cells, suggesting that the SH3 domains of CIN85 are required for its association with Cbl and BLNK. Because the tyrosine phosphorylation of c-Cbl and BLNK is critical for their function,^{6,27} we next determined whether the overexpression of WT and SH3-deleted CIN85 affects BCR-induced phosphorylation of c-Cbl and BLNK. Compared with control cells, WT and SH3-deleted CIN85 sustained and inhibited c-Cbl phosphorylation, respectively (Figure 1B). In addition, WT and SH3-deleted CIN85 inhibited and enhanced BLNK phosphorylation, respectively (Figure 1B). These findings

suggest that CIN85 associates with Cbl and BLNK and regulates their phosphorylation in an opposite manner.

Forced CIN85 expression inhibits BCR-induced calcium flux and the phosphorylation of Syk and PLCγ2

We tested whether the overexpression of WT and SH3-deleted CIN85 affects early BCR signaling. Syk phosphorylation, which is one of the earliest events in BCR signaling, was inhibited in WT CIN85-expressing cells, whereas it was sustained in SH3-deleted CIN85-expressing cells (Figure 2A-B). Two enzymes, PLCγ2 and PI3K, function as critical mediators downstream of BCR signaling.^{1,2,28} WT and SH3-deleted CIN85 partially inhibited and enhanced BCR-induced phosphorylation of PLCγ2, respectively (Figure 2A-B). In contrast, the phosphorylation of Akt, which is a downstream molecule of PI3K, was not affected in WT or SH3-deleted CIN85-expressing cells (Figure 2A). Activated PLCγ2 converts PIP2 into IP3 and diacylglycerol, of which PIP2 is critical for calcium flux in B cells.^{1,2,12} Consistent with the levels of PLCγ2 phosphorylation, the BCR-induced calcium flux was significantly inhibited in WT CIN85-expressing cells, whereas it was slightly sustained in SH3-deleted CIN85-expressing cells (Figure 2C). These results suggest that CIN85 inhibits BCR-induced calcium flux and the

phosphorylation of Syk and PLC γ 2, and that the SH3 domains of CIN85 are required for its inhibitory function.

CIN85 knockdown enhances BCR-induced calcium flux and the phosphorylation of Syk, Vav2, and PLC γ 2, leading to augmented NF-AT activation and CD69 expression

To elucidate the role of endogenously expressed CIN85 in BCR signaling, we generated CIN85-knockdown B cell lines. In contrast to the CIN85-overexpressing cells (Figures 1 and 2), CIN85-knockdown cells exhibited enhanced phosphorylation of Syk, BLNK, and PLC γ 2 (Figure 3A-B). Akt phosphorylation was comparable between control and CIN85-knockdown cells (Figure 3A). Consistent with the levels of PLC γ 2 phosphorylation, BCR-induced calcium flux was accentuated in CIN85-knockdown cells (Figure 3C). Vav2 positively regulates PLC γ 2 activation in B cells.²⁹ Vav2 phosphorylation was enhanced in CIN85-knockdown cells (Figure 3D). These BCR signaling profiles in CIN85-knockdown cells are reminiscent of those in c-Cbl/Cbl-b double-knockout B cells.¹⁰ The phosphorylation of c-Cbl was significantly inhibited in CIN85-knockdown cells (Figure 3E). BCR-induced calcium flux plays a crucial role in the activation of the transcription factor NF-AT, the disruption of which results in significant defects in B-cell function.³⁰ BCR-induced NF-AT activation was enhanced in CIN85-knockdown cells (Figure 3F). In addition, BCR-induced up-regulation of the activation marker CD69 was pronounced in CIN85-knockdown cells (Figure 3G). These phenotypes in CIN85-knockdown cells were again similar to those observed in Cbl-deficient B cells.¹⁰ Given that CIN85 strongly associates with Cbl proteins (Figure 1A), these results suggest that CIN85 plays a vital role in Cbl-mediated regulation of BCR signaling.

CIN85 promotes the ubiquitination and degradation of Syk in B cells

Cbl proteins function as E3 ubiquitin ligases and target PTK substrates, including Syk, for degradation.^{31,32} We thus tested whether CIN85 affects Syk ubiquitination in B cells. Syk ubiquitination was induced on BCR stimulation. Compared with control cells, Syk ubiquitination was increased in WT CIN85-expressing cells (Figure 4A). In contrast, an impairment in Syk ubiquitination was noted in CIN85-knockdown cells (Figure 4A). These results suggest that CIN85 positively regulates Cbl-mediated ubiquitination of BCR-signaling molecules including Syk. Despite the altered levels of Syk ubiquitination, the level of total Syk protein was not altered in the WT CIN85-expressing or CIN85-knockdown cells throughout the stimulation (Figures 2A and 3A). Because only a small pool of Syk is phosphorylated on stimulation and targeted for degradation in B cells,³¹ we tested the degree of Syk phosphorylation among the total Syk immunoprecipitate. The levels of phosphorylated Syk were reduced in WT CIN85-expressing cells but enhanced in CIN85-knockdown cells (Figure 4B), suggesting that CIN85 promotes Cbl-dependent loss of the phosphorylated pool of Syk in B cells.

CIN85 does not affect BCR internalization

CIN85 regulates Cbl-mediated internalization of the EGFR in several cell types other than B cells.^{18,19} To test whether CIN85 affects BCR internalization, we first monitored the levels of surface BCR expression after stimulation. Without stimuli, the levels of surface BCR were similar on CIN85 overexpression and CIN85 knockdown. In parental cells, BCR crosslinking caused a rapid decrease in surface BCR levels, suggesting that BCR was efficiently internalized after stimulation

(Figure 5A; supplemental Figure 1A, available on the *Blood* Web site; see the Supplemental Materials link at the top of the online article). BCR internalization was not affected in the WT or SH3-deleted CIN85-expressing cells. Moreover, the absence of endogenous CIN85 did not affect BCR internalization (Figure 5B, supplemental Figure 1A). Next, we directly visualized BCRs in B cell lines using fluorescence microscopy. In control cells, the BCR complexes exhibited a slightly patchy distribution before stimulation, and within 3 minutes after stimulation, the BCRs formed polarized tight caps on the cell surface. After 10 minutes of BCR stimulation, a punctate pattern of internalized BCRs was clearly visualized (Figure 5C). Consistent with the findings obtained with flow cytometry (Figure 5A-B), the spatial and temporal distribution of BCR complexes in CIN85-overexpressing and CIN85-knockdown cells appeared similar to that in control cells (Figure 5C, supplemental Figure 1B-C). These findings suggest that CIN85 does not affect BCR internalization.

CIN85 knockdown enhances the survival, growth, and differentiation of primary B cells

BCR signaling plays a critical role in determining the survival, growth, and differentiation of B cells.¹ It was thus of interest to test whether CIN85 affects B cell fate. A major obstacle, however, is that the survival, growth, and differentiation of B cell cannot be properly assessed in transformed B cells. We therefore sought to knock down CIN85 expression in human primary B cells. After introduction of the GFP-CIN85 knockdown vector, GFP-positive B cells were sorted and used for further experimentation. Under these conditions, we were able to knock down the CIN85 mRNA expression in B cells by 60%-80% (Figure 6A).

We first tested whether CIN85 knockdown affects the expression of the B-cell survival-associated genes Bcl_xL and A1. Consistent with previous studies,³³ BCR stimulation induced Bcl_xL and A1 mRNA expression in control cells. This induction was far more drastic in CIN85-knockdown B cells (Figure 6A). The costimulation of TLR9 with its ligand CpG enhances BCR-induced expression of B-cell survival genes.³⁴ This enhancement was less evident in CIN85-knockdown cells than in control cells (Figure 6A), suggesting that CIN85 knockdown requires less costimulation for the full induction of B-cell survival genes. Consistent the findings for the transcript levels, the BCR-induced expression of Bcl_xL protein was more pronounced in CIN85-knockdown cells (Figure 6B). We also tested whether CIN85 knockdown affects BCR-induced death of B cells using the annexin-binding assay. The CIN85-knockdown cells exhibited less BCR-induced cell death (Figure 6C). We next tested whether CIN85 knockdown affects the expression of the B-cell growth-associated genes cyclin D2 and myc. Again, BCR-induced expression of these genes was more pronounced in CIN85-knockdown cells (Figure 6A), and costimulation with TLR9 did not enhance induction compared with the control cells. Consistent with the findings for the transcript levels, BCR-induced expression of cyclin D2 protein was more pronounced in CIN85-knockdown cells (Figure 6B). We also tested whether CIN85 knockdown affects B-cell growth using the BrdU uptake assay. Consistent with the expression levels of cyclin D2 and myc, CIN85 knockdown enhanced BCR-induced cell growth (Figure 6D). On activation, B cells undergo plasma cell differentiation along with the expression of critical differentiation-associated genes such as Blimp-1 and Xbp-1. Consistent with previous studies,³⁵ BCR stimulation alone was not sufficient to induce the expression of Blimp-1 and Xbp-1 in human B cells (data not shown). However, the combined stimulation of BCR and TLR9 clearly induced the expression of these genes in control cells,

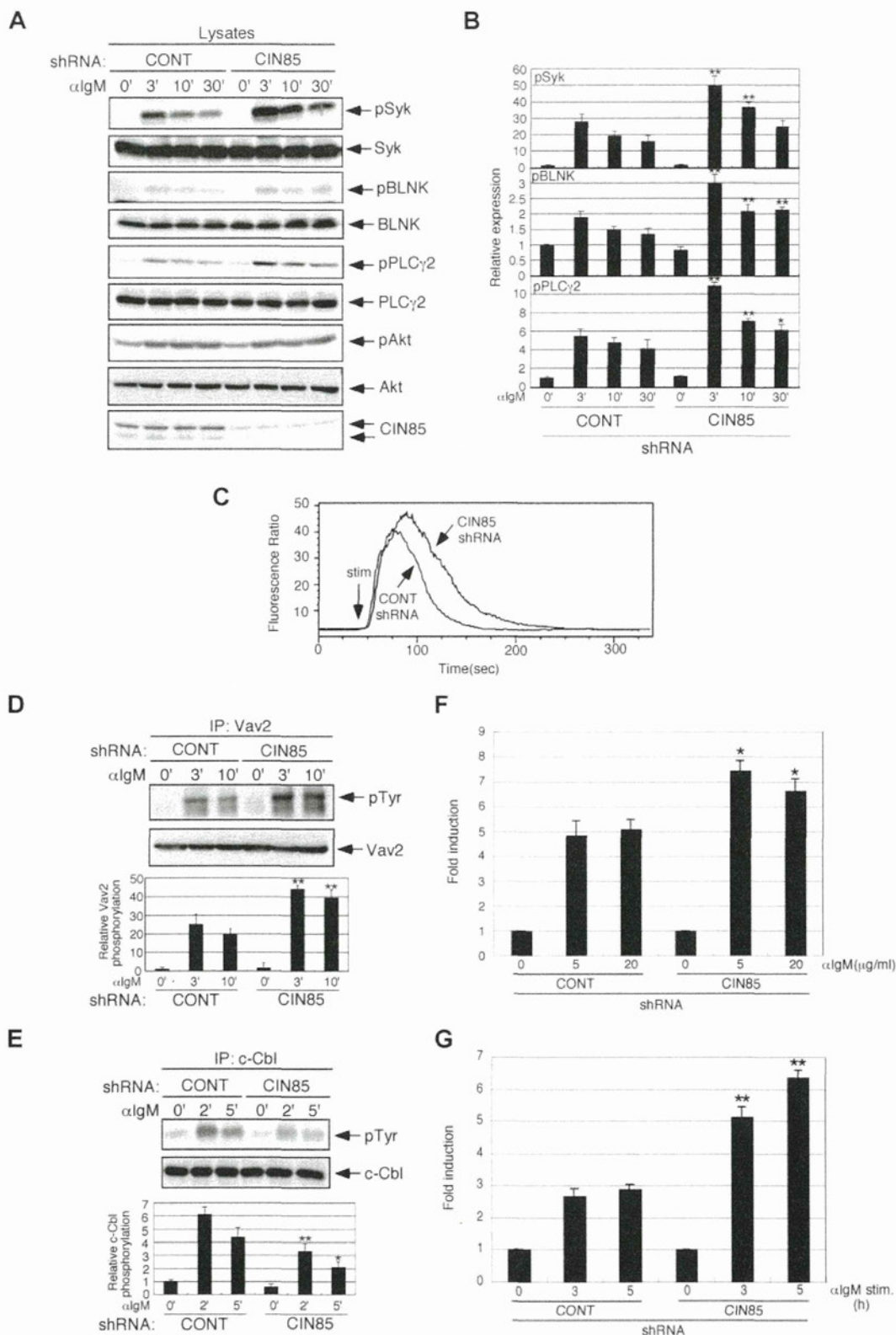
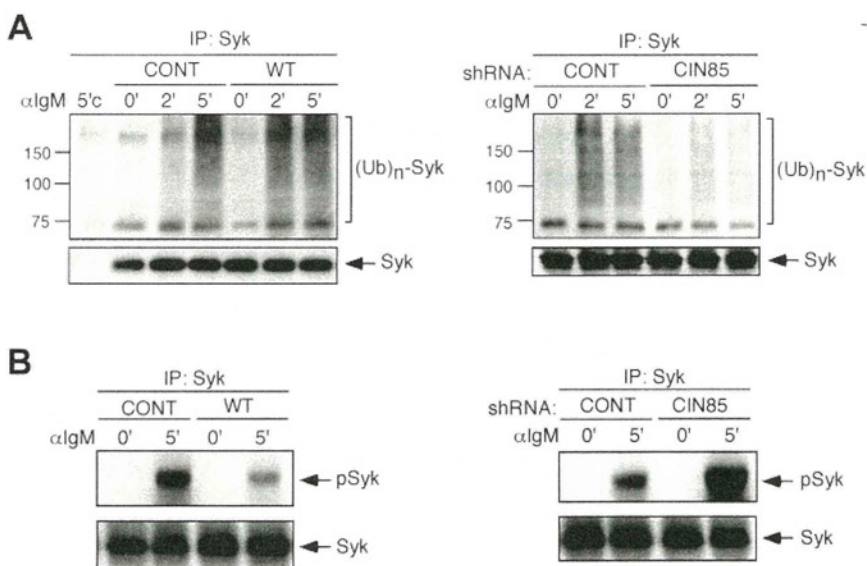


Figure 3. CIN85 knockdown enhances BCR-induced calcium flux and phosphorylation of Syk, Vav2, and PLCγ2, leading to augmented NF-AT activation and CD69 expression. (A-B) Stable control and CIN85-knockdown B220 cells were stimulated with 20 μg/mL F(ab')₂ goat anti-human IgM for the indicated time periods. The cell lysates were subsequently separated on a 10% SDS-PAGE gel and analyzed by Western blotting with anti-phospho-Syk pAb, anti-Syk mAb, anti-phospho-BLNK mAb, anti-BLNK mAb, anti-phospho-PLCγ2 pAb, anti-PLCγ2 pAb, anti-phospho-Akt pAb, anti-Akt pAb, or anti-CIN85 mAb. The resulting values are expressed as fold changes in protein expression compared with unstimulated control cells. The values are the mean ± SD of 3 independent experiments (**P* < .05, ***P* < .01 vs controls). (C) Ca²⁺ influx in stable control and CIN85-knockdown B220 cells. Intracellular free calcium levels in Fluo 4/AM-loaded cells were analyzed using flow cytometry after the cells were stimulated with 20 μg/mL F(ab')₂ goat anti-human IgM. The results shown are representative of 4 independent experiments. (D-E) Stable control and CIN85-knockdown B220 cells were stimulated with 20 μg/mL F(ab')₂ goat anti-human IgM for the indicated time periods. Immunoprecipitates with anti-Vav2 or anti-c-Cbl mAb were separated on a 10% SDS-PAGE gel and analyzed by Western blotting with anti-phosphotyrosine mAb, anti-Vav2 mAb, or anti-c-Cbl mAb. The resulting values are expressed as fold changes in protein expression compared with unstimulated control cells. The values are the mean ± SD of 3 independent experiments (**P* < .05, ***P* < .01 vs controls). (F) Stable control

Figure 4. CIN85 promotes Syk ubiquitination and degradation in B cells. (A) Control BJAB cells, stable transformants expressing WT CIN85, and CIN85-knockdown BJAB cells were stimulated with 20 μ g/mL F(ab')₂ goat anti-human IgM for the indicated time periods. Immunoprecipitates with anti-Syk mAb were separated on a 10% SDS-PAGE gel and analyzed by Western blotting with anti-ubiquitin or anti-Syk mAb. 5'c, immunoprecipitation of the cell lysates at 5 minutes with isotype control. The molecular weight is indicated on the left side of the blots. (B) Control BJAB cells, stable transformants expressing WT CIN85, and CIN85-knockdown BJAB cells were stimulated with 20 μ g/mL F(ab')₂ goat anti-human IgM for 5 minutes. Immunoprecipitates with anti-Syk mAb were separated on a 10% SDS-PAGE gel and analyzed by Western blotting with anti-phospho-Syk pAb or anti-Syk mAb.



whereas this induction was more pronounced in CIN85-knockdown B cells (Figure 6E). Consistent with the findings for the transcript levels, BCR stimulation alone did not induce detectable levels of Blimp-1 protein. However, the combined stimulation of BCR and TLR9 clearly induced the expression of the Blimp-1 protein in control cells, although this was more pronounced in CIN85-knockdown cells (Figure 6F). These results suggest that CIN85 is required for Cbl-mediated regulation of BCR signaling and downstream events such as the survival, growth, and differentiation of human B cells.

Discussion

We demonstrated here that CIN85 functions as a novel adaptor to regulate proximal BCR signaling. Gain-of-function and loss-of-function experiments revealed that CIN85 not only enhances BCR-induced c-Cbl phosphorylation but also inhibits BCR-induced calcium flux and the phosphorylation of Syk and PLC γ 2. CIN85 promotes c-Cbl-dependent ubiquitination and degradation of Syk, which is a key upstream kinase that propagates BCR signaling by phosphorylating downstream molecules including PLC γ 2. Because Cbl proteins directly associate with Syk and inhibit its function,⁶ it is probable that CIN85 acts as a critical scaffolding adaptor for Cbl proteins and is indispensable for Cbl-mediated regulation of Syk activation in B cells.

Consistent with our findings, a critical role of CIN85 in Cbl-mediated regulation of Syk activation was recently shown in Fc ϵ RI signaling in mast cells.²¹ In mast cells, CIN85 enhances c-Cbl-mediated ubiquitination and the degradation of Syk protein.²¹ In B cells, however, CIN85 overexpression significantly increased Syk ubiquitination (Figure 4), but CIN85 knockdown did not alter the total levels of Syk protein throughout stimulation (Figure 3A), as previously shown in c-Cbl/Cbl-b double-knockout B cells.¹⁰ This apparent discrepancy in Syk degradation between

mast cells and B cells could be explained by the findings of Rao et al.,³¹ who showed that on BCR stimulation, only a small portion of Syk is phosphorylated and then degraded by c-Cbl. Rao et al also showed that c-Cbl does not directly affect the catalytic activity of Syk.³¹ Consistent with these findings, our study showed that CIN85 promotes c-Cbl-mediated ubiquitination and degradation of the phosphorylated pool of Syk (Figure 4A-B).

What, then, are the possible mechanisms by which CIN85 enhances BCR-induced c-Cbl phosphorylation in B cells? Src-family PTKs and Syk are proposed to phosphorylate c-Cbl on tyrosines.⁶ We previously showed that CIN85 directly interacts with the SH3 domain of Src-family PTKs including Lyn.¹⁷ In addition, CIN85 directly associates with BLNK, PLC γ and Vav, all of which are direct Syk interactors,^{17,36} and thus, CIN85 is indirectly associated with Syk via binding to BLNK, PLC γ , and Vav. In view of these findings, it seems probable that CIN85 acts as a key scaffolding adaptor that permits the spatial proximity of Src-family PTKs, Syk, and Cbl proteins and thus facilitates their phosphorylation of Cbl proteins.

Although CIN85 appears to function in concert with Cbl proteins to regulate BCR signaling, an additional mechanism is possible. Previous *in vitro* binding experiments showed that CIN85 directly binds to Src-family tyrosine kinases, PLC γ , p85 PI3K, Vav, Btk, and SHIP, all of which are involved in BCR signaling, through its SH3 domains and proline-rich region.^{15,24,25} In addition, a recent study showed that the SH3 domains of CIN85 could uniquely bind to ubiquitin.³⁷ Thus, after various BCR-signaling molecules are ubiquitinated by Cbl proteins on stimulation, the competition between canonical SH3 ligands and ubiquitin binding to CIN85 may affect BCR signaling in a temporal and spatial manner. Therefore, it is probable that CIN85 also directly regulates BCR signaling by a Cbl-independent mechanism.

A recent study using liquid chromatography-coupled tandem mass spectrometry showed that 3 SH3 domains of CIN85 could recruit protein molecules required for the proper formation and

Figure 3 (continued) and CIN85-knockdown BJAB cells transfected with the NF-AT luciferase reporter construct were stimulated with graded doses of F(ab')₂ goat anti-human IgM for 8 hours and lysed, and the luciferase activity was assayed using a luminometer. The relative luciferase activity of the medium and BCR-stimulated cells was expressed with respect to that of the PMA/ionomycin stimulation. The results were presented as the mean and SEM of triplicate cultures. One experiment representative of 4 independent experiments is shown (**P* < .05 vs controls). (G) Stable control and CIN85-knockdown BJAB cells before and after stimulation with 20 μ g/mL F(ab')₂ goat anti-human IgM (3 and 5 hours) were analyzed for surface expression of CD69. One experiment representative of 3 independent experiments is shown (***P* < .01 vs controls).

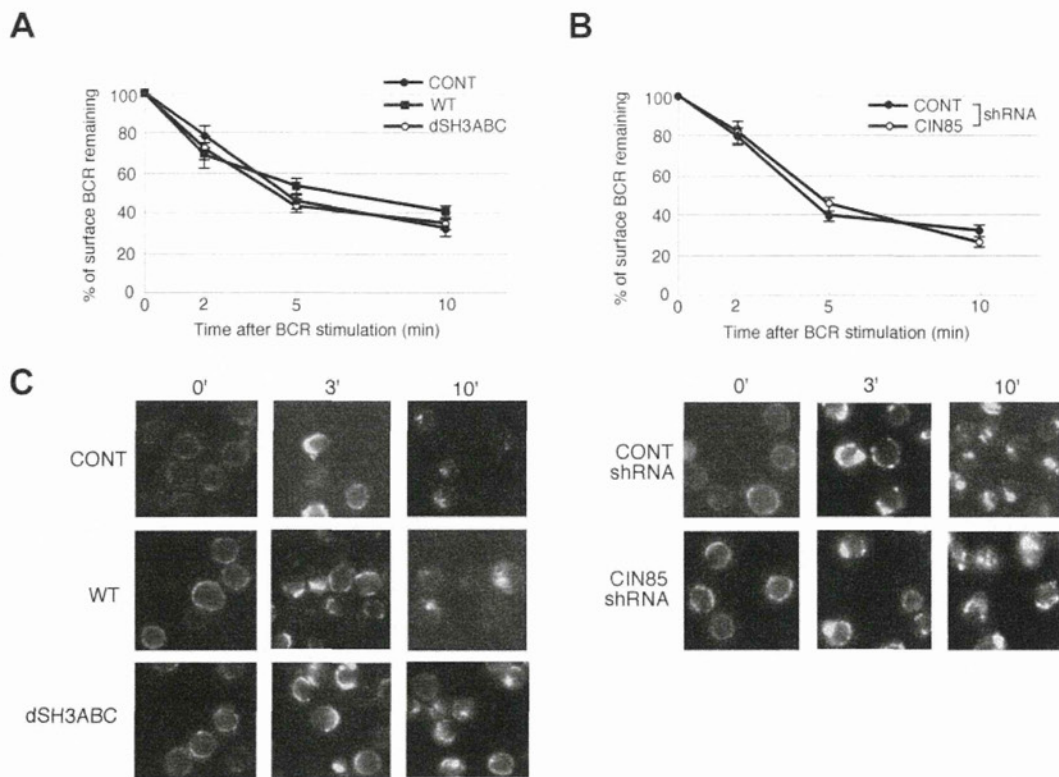


Figure 5. CIN85 does not affect BCR internalization. (A) BJAB cells (control and stable transformants expressing either WT or SH3-deleted CIN85) and (B) BJAB cells (control and CIN85-knockdown) were incubated at 4°C with F(ab')₂ goat anti-human IgM for 30 minutes. The cells were washed, warmed to 37°C for the indicated time intervals, stained at 4°C for 30 minutes with a FITC-labeled anti-goat IgG pAb, and analyzed by flow cytometry. The results are expressed as the percentage of surface BCRs remaining. The data are presented as the average and SEM of 3 independent experiments. (C) Control BJAB cells, stable transformants expressing either WT or SH3-deleted CIN85, and CIN85-knockdown BJAB cells were incubated at 4°C with 20 μg/mL F(ab')₂ goat anti-human IgM for 30 minutes. The cells were washed and warmed to 37°C for the indicated time periods. The cells were fixed, permeabilized, stained with a FITC-labeled anti-goat IgG pAb, and analyzed by fluorescence microscopy. The images shown are representative of 3 independent experiments.

function of coated vesicles.²⁵ Similarly, early studies showed a characteristic feature of CIN85 in the formation of clathrin-coated vesicles during the internalization of RTKs such as EGFRs in nonimmune cells.^{18,19} Brain-specific CIN85-deficient mice manifest impaired internalization of D2 dopamine receptors, which belong to the 7-transmembrane G protein-coupled receptor superfamily.³⁸ In addition, CIN85 facilitates ligand-induced FcεRI internalization in RBL-2H3 mast cell lines.²⁰ Because BCR internalization is regulated via a clathrin-dependent pathway,³⁹ it was of interest to determine whether CIN85 regulates BCR internalization. Our study, however, shows that CIN85 does not affect BCR internalization (Figure 5, supplemental Figure 1). These data are somewhat surprising, given that Cbl proteins control BCR internalization by a ubiquitin-dependent mechanism.^{10,40} However, the role of Cbl proteins in BCR ubiquitination and internalization is still rather controversial. The HECT family member Itch, but not c-Cbl, is an E3 ubiquitin ligase that is involved in BCR ubiquitination.⁴¹ In addition, the ubiquitination of Igβ, which is a component of BCR, does not facilitate BCR internalization but is required for the sorting of early endosomes and for trafficking into late endosomes,⁴¹ which suggests that BCR ubiquitination is more critical at the later stage of its trafficking. Because our imaging analysis (Figure 5C) cannot clearly distinguish the spatial distribution of early and late endosomes, it is of great interest to test whether CIN85 affects postendocytotic BCR trafficking. A recent study showed that in human neutrophils, CIN85 modulates c-Cbl-mediated down-regulation of FcγRIIIa in the later stages of receptor trafficking without affecting the internalization of this receptor.²²

During the submission of this paper, 2 studies were published that, in contrast to our findings, showed that CIN85 positively regulates BCR signaling in mouse and chicken B cells.^{42,43} These studies found that CIN85 associates with BLNK and regulates BCR-induced NF-κB activation. However, the detailed profiles of BCR signaling differ between the 2 studies: the BCR-induced phosphorylation of BLNK and PLCγ2 and the calcium flux are significantly decreased on the loss of CIN85 in chicken B cells, whereas they are apparently normal in CIN85-deficient mouse B cells.^{42,43} It should be noted that the former study did not actually use CIN85-deficient cells; rather, it used cells expressing a mutant BLNK that failed to bind to CIN85 or its homolog CD2AP.⁴² Although these findings are intriguing, it is rather surprising that Cbl-mediated function of CIN85 in B cells was barely investigated in these studies. As previously mentioned, it is becoming evident that Cbl proteins play a critical role in the function of CIN85 in immune cells.²⁰⁻²² In addition, BCR-induced association of CIN85 with c-Cbl was recently shown even in mouse B cells.⁴⁴ We thus find that in human B cells, CIN85 negatively regulates BCR signaling via a Cbl-dependent mechanism. Our data obtained using CIN85-knockdown primary B cells also support this hypothesis. The molecular reason underlying the apparent discrepancy between our study and the aforementioned ones^{42,43} remains unclear. One possibility, however, is that the relative contribution of CIN85-binding partners varies depending on the source of B cells used. In human B cells, Cbl proteins seem to preferentially associate with CIN85 over BLNK (Figure 1A). Notably, we found that CD2AP seems to preferentially associate with BLNK over c-Cbl in human B cells (supplemental Figure 2). It is therefore of potential interest

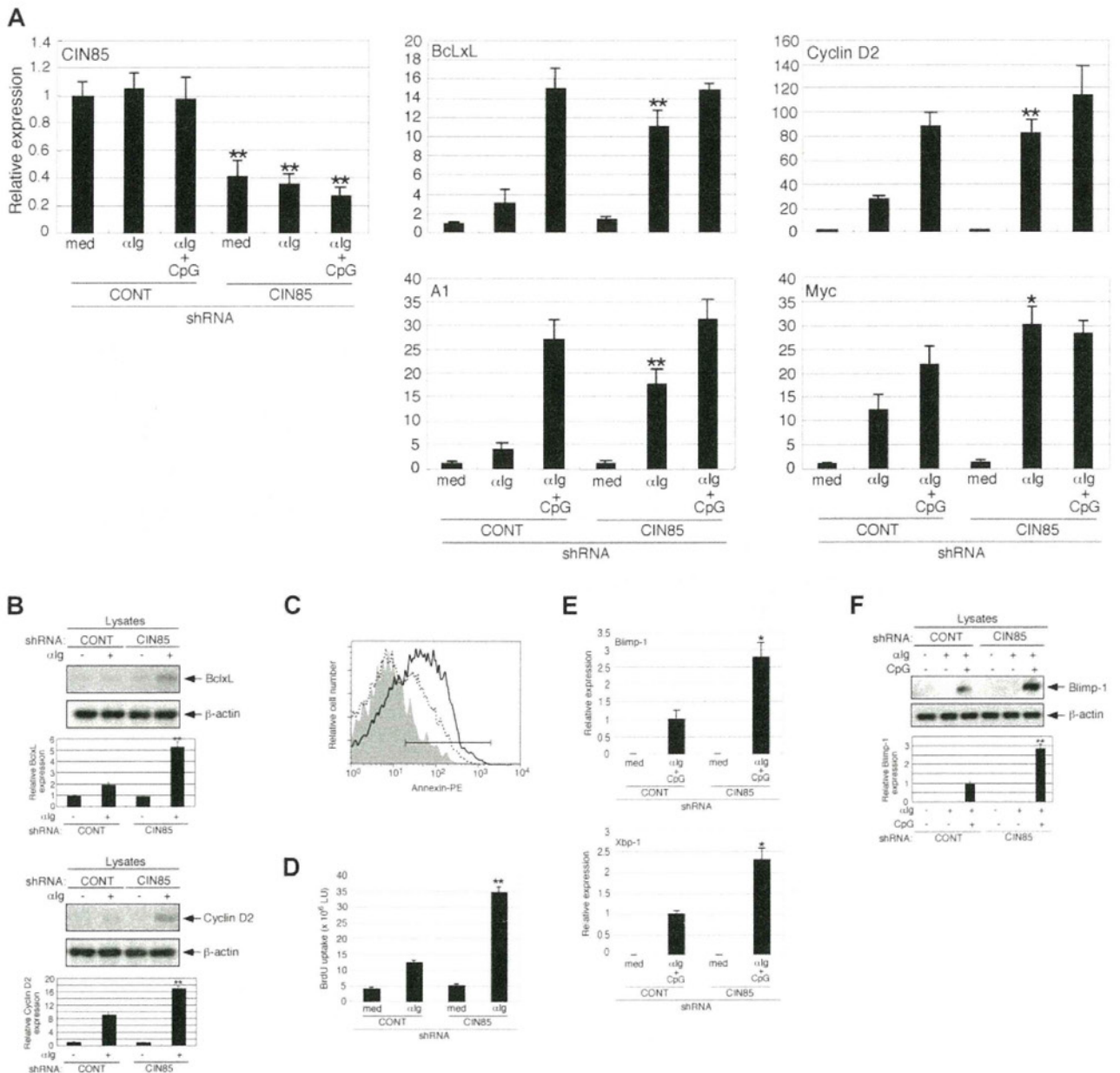


Figure 6. CIN85 knockdown enhances the survival, growth, and differentiation of primary B cells. (A) Control and CIN85-knockdown primary B cells were incubated for 24 hours in medium containing F(ab')₂ goat anti-human IgG/IgA/IgM (α Ig, 20 μ g/mL) or α Ig plus CpG (1 μ M), and CIN85, BclxL, A1, cyclin D2, and myc mRNA levels were quantified by real-time PCR. The data are normalized to the expression of 18S rRNA. The results shown are representative of 3 independent experiments (**P* < .05, ***P* < .01 vs controls). (B) Control and CIN85-knockdown primary B cells were incubated for 24 hours in the absence or presence of F(ab')₂ goat anti-human IgG/IgA/IgM (α Ig, 20 μ g/mL). The cell lysates were subsequently separated on a SDS-PAGE gel and analyzed by Western blotting with anti-BclxL mAb, anti-cyclin D2 pAb, or anti- β -actin mAb. The resulting values are expressed as fold changes in protein expression compared with nonstimulated control cells. The values are the mean \pm SD of 3 independent experiments (***P* < .01 vs controls). (C) Control and CIN85-knockdown primary B cells were incubated for 48 hours in the absence or presence of F(ab')₂ goat anti-human IgG/IgA/IgM (α Ig, 20 μ g/mL). After culture, the cells were stained with PE-labeled annexin V and analyzed using flow cytometry. The percentages of annexin-positive cells are shown. A representative histogram of 3 independent experiments is shown. (D) Control and CIN85-knockdown primary B cells were incubated for 48 hours in the absence or presence of F(ab')₂ goat anti-human IgG/IgA/IgM (α Ig, 20 μ g/mL). After culture, the cells were pulsed with BrdU, and its incorporation was detected by incubation with anti-BrdU mAb, followed by rhodamine-conjugated anti-mouse Ab. A representative histogram of 3 independent experiments is shown (***P* < .01 vs controls). (E) Control and CIN85-knockdown primary B cells were incubated for 48 hours in the absence or presence of F(ab')₂ goat anti-human IgG/IgA/IgM (α Ig, 20 μ g/mL) and CpG (1 μ M), and quantitation of Blimp-1 and Xbp-1 mRNA by real-time PCR was carried out. The data are normalized to the expression of 18S rRNA. The results shown are representative of 3 independent experiments (**P* < .05 vs controls). (F) Control and CIN85-knockdown primary B cells were incubated for 48 hours with or without F(ab')₂ goat anti-human IgG/IgA/IgM (α Ig, 20 μ g/mL) in the absence or presence of CpG (1 μ M). The cell lysates were subsequently separated on a SDS-PAGE gel and analyzed by Western blotting with anti-Blimp-1 mAb or anti- β -actin mAb. The resulting values are expressed as fold changes in protein expression compared with unstimulated control cells. The values are the mean \pm SD of 3 independent experiments (***P* < .01 vs controls).

to compare the roles of CIN85 and CD2AP in the function of human B cells.

BCR signals play a pivotal role in the survival, growth, and differentiation of B cells.^{1,2} Under physiologic conditions, BCR signaling is fine-tuned by positive and negative regulators and is

generally insufficient for the full activation of B cells, rendering them susceptible to apoptosis and anergy. However, when the negative regulation of BCR signaling is compromised, unwanted B cells could grow and survive, thereby potentially leading to autoimmunity and B-cell malignancies. This study showed that

CIN85 knockdown in primary B cells causes full activation of B cells and enhances BCR-induced survival and growth via the increased expression of BclLxL, A1, cyclin D2, and myc (Figure 6). Given that Cbl proteins are critical for B-cell anergy,¹⁰ CIN85 may cooperate with Cbl proteins to function as a key negative regulator for BCR signaling and to maintain self-tolerance. It is thus of interest to determine whether the expression and/or function of CIN85 could be altered in human autoimmune diseases such as SLE. Surprisingly, CLL cells from advanced-stage patients exhibit hypophosphorylation of c-Cbl,¹¹ as seen in CIN85-knockdown cells. The manipulation of CIN85 expression may therefore provide a novel strategy to control aberrant cell growth and survival in B-cell malignancies.

Acknowledgments

The authors thank Editage for proofreading the English used in this paper.

References

- Nihiro H, Clark EA. Regulation of B-cell fate by antigen-receptor signals. *Nat Rev Immunol*. 2002;2(12):945-956.
- Kurosaki T, Shinohara H, Baba Y. B cell signaling and fate decision. *Annu Rev Immunol*. 2010;28:21-55.
- Pogue SL, Kurosaki T, Bolen J, Herbst R. B cell antigen receptor-induced activation of Akt promotes B cell survival and is dependent on Syk kinase. *J Immunol*. 2000;165(3):1300-1306.
- Thien CB, Langdon WY. c-Cbl and Cbl-b ubiquitin ligases: substrate diversity and the negative regulation of signalling responses. *Biochem J*. 2005;391(pt 2):153-166.
- Liu YC, Gu H. Cbl and Cbl-b in T-cell regulation. *Trends Immunol*. 2002;23(3):140-143.
- Swaminathan G, Tsygankov AY. The Cbl family proteins: ring leaders in regulation of cell signalling. *J Cell Physiol*. 2006;209(1):21-43.
- Duan L, Reddi AL, Ghosh A, Dimri M, Band H. The Cbl family and other ubiquitin ligases: destructive forces in control of antigen receptor signaling. *Immunity*. 2004;21(1):7-17.
- Panchamoorthy G, Fukazawa T, Miyake S, et al. p120cbl is a major substrate of tyrosine phosphorylation upon B cell antigen receptor stimulation and interacts in vivo with Fyn and Syk tyrosine kinases, Grb2 and Shc adaptors, and the p85 subunit of phosphatidylinositol 3-kinase. *J Biol Chem*. 1996;271(6):3187-3194.
- Yasuda T, Maeda A, Kurosaki M, et al. Cbl suppresses B cell receptor-mediated phospholipase C (PLC)-gamma2 activation by regulating B cell linker protein-PLC-gamma2 binding. *J Exp Med*. 2000;191(4):641-650.
- Kitaura Y, Jang IK, Wang Y, et al. Control of the B cell-intrinsic tolerance programs by ubiquitin ligases Cbl and Cbl-b. *Immunity*. 2007;26(5):567-578.
- Mankai A, Eveillard JR, Buhe V, et al. Is the c-Cbl proto-oncogene involved in chronic lymphocytic leukemia? *Ann N Y Acad Sci*. 2007;1107:193-205.
- Nihiro H, Maeda A, Kurosaki T, Clark EA. The B lymphocyte adaptor molecule of 32 kD (Bam32) regulates B cell antigen receptor signaling and cell survival. *J Exp Med*. 2002;195(1):143-149.
- Nihiro H, Allam A, Stoddart A, Brodsky FM, Marshall AJ, Clark EA. The B lymphocyte adaptor molecule of 32 kilodaltons (Bam32) regulates B cell antigen receptor internalization. *J Immunol*. 2004;173(9):5601-5609.
- Take H, Watanabe S, Takeda K, Yu ZX, Iwata N, Kajigaya S. Cloning and characterization of a novel adaptor protein, CIN85, that interacts with c-Cbl. *Biochem Biophys Res Commun*. 2000;268(2):321-328.
- Gout I, Middleton G, Adu J, et al. Negative regulation of PI 3-kinase by Ruk, a novel adaptor protein. *EMBO J*. 2000;19(15):4015-4025.
- Bogler O, Furnari FB, Kindler-Roehrborn A, et al. SETA: a novel SH3 domain-containing adapter molecule associated with malignancy in astrocytes. *Neuro Oncol*. 2000;2(1):6-15.
- Narita T, Amano F, Yoshizaki K, et al. Assignment of SH3KBP1 to human chromosome band Xp22.1->p21.3 by in situ hybridization. *Cytogenet Cell Genet*. 2001;93(1-2):133-134.
- Petrelli A, Gilestro GF, Lanzardo S, Comoglio PM, Migone N, Giordano S. The endophilin-CIN85-Cbl complex mediates ligand-dependent downregulation of c-Met. *Nature*. 2002;416(6877):187-190.
- Soubeyran P, Kowanetz K, Szymkiewicz I, Langdon WY, Dikic I. Cbl-CIN85-endophilin complex mediates ligand-induced downregulation of EGF receptors. *Nature*. 2002;416(6877):183-187.
- Molfetta R, Belleudi F, Peruzzi G, et al. CIN85 regulates the ligand-dependent endocytosis of the IgE receptor: a new molecular mechanism to dampen mast cell function. *J Immunol*. 2005;175(7):4208-4216.
- Peruzzi G, Molfetta R, Gasparini F, et al. The adaptor molecule CIN85 regulates Syk tyrosine kinase level by activating the ubiquitin-proteasome degradation pathway. *J Immunol*. 2007;179(4):2089-2096.
- Marois L, Vaillancourt M, Pare G, et al. CIN85 modulates the down-regulation of Fc gammaRIIIa expression and function by c-Cbl in a PKC-dependent manner in human neutrophils. *J Biol Chem*. 2011;286(17):15073-15084.
- Tabrizi SJ, Nihiro H, Masui M, et al. T cell leukemia/lymphoma 1 and galectin-1 regulate survival/cell death pathways in human naive and IgM+ memory B cells through altering balances in Bcl-2 family proteins. *J Immunol*. 2009;182(3):1490-1499.
- Narita T, Nishimura T, Yoshizaki K, Taniyama T. CIN85 associates with TNF receptor 1 via Src and modulates TNF-alpha-induced apoptosis. *Exp Cell Res*. 2005;304(1):256-264.
- Havrylov S, Rzhetsky Y, Malinowska A, Drobot L, Redowicz MJ. Proteins recruited by SH3 domains of Ruk/CIN85 adaptor identified by LC-MS/MS. *Proteome Sci*. 2009;7:21.
- Watanabe S, Take H, Takeda K, Yu ZX, Iwata N, Kajigaya S. Characterization of the CIN85 adaptor protein and identification of components involved in CIN85 complexes. *Biochem Biophys Res Commun*. 2000;278(1):167-174.
- Chiu CW, Dalton M, Ishiai M, Kurosaki T, Chan AC. BLNK: molecular scaffolding through 'cis'-mediated organization of signaling proteins. *EMBO J*. 2002;21(23):6461-6472.
- Marshall AJ, Nihiro H, Yun TJ, Clark EA. Regulation of B-cell activation and differentiation by the phosphatidylinositol 3-kinase and phospholipase Cgamma pathway. *Immunol Rev*. 2000;176:30-46.
- Turner M. B-cell development and antigen receptor signalling. *Biochem Soc Trans*. 2002;30(4):812-815.
- Peng SL, Gerth AJ, Ranger AM, Glimcher LH. NFATc1 and NFATc2 together control both T and B cell activation and differentiation. *Immunity*. 2001;14(1):13-20.
- Rao N, Ghosh AK, Ota S, et al. The non-receptor tyrosine kinase Syk is a target of Cbl-mediated ubiquitination upon B-cell receptor stimulation. *EMBO J*. 2001;20(24):7085-7095.
- Sohn HW, Gu H, Pierce SK. Cbl-b negatively regulates B cell antigen receptor signaling in mature B cells through ubiquitination of the tyrosine kinase Syk. *J Exp Med*. 2003;197(11):1511-1524.
- Su TT, Rawlings DJ. Transitional B lymphocyte subsets operate as distinct checkpoints in murine splenic B cell development. *J Immunol*. 2002;168(5):2101-2110.
- Yi AK, Chang M, Peckham DW, Krieg AM, Ashman RF. CpG oligodeoxynucleotides rescue mature spleen B cells from spontaneous apoptosis and promote cell cycle entry. *J Immunol*. 1998;160(12):5898-5906.
- Calame KL, Lin KI, Tunyaplin C. Regulatory mechanisms that determine the development and function of plasma cells. *Annu Rev Immunol*. 2003;21:205-230.
- Turner M, Schweighoffer E, Colucci F, Di Santo JP, Tybulewicz VL. Tyrosine kinase SYK: essential functions for immunoreceptor signalling. *Immunol Today*. 2000;21(3):148-154.

37. Stamenova SD, French ME, He Y, Francis SA, Kramer ZB, Hicke L. Ubiquitin binds to and regulates a subset of SH3 domains. *Mol Cell*. 2007; 25(2):273-284.
38. Shimokawa N, Haglund K, Holter SM, et al. CIN85 regulates dopamine receptor endocytosis and governs behaviour in mice. *EMBO J*. 2010; 29(14):2421-2432.
39. Stoddart A, Dykstra ML, Brown BK, Song W, Pierce SK, Brodsky FM. Lipid rafts unite signaling cascades with clathrin to regulate BCR internalization. *Immunity*. 2002;17(4):451-462.
40. Jacob M, Todd L, Sampson MF, Pure E. Dual role of Cbl links critical events in BCR endocytosis. *Int Immunol*. 2008;20(4):485-497.
41. Zhang M, Veselits M, O'Neill S, et al. Ubiquitylation of Ig beta dictates the endocytic fate of the B cell antigen receptor. *J Immunol*. 2007;179(7): 4435-4443.
42. Oellerich T, Bremes V, Neumann K, et al. The B-cell antigen receptor signals through a pre-formed transducer module of SLP65 and CIN85. *EMBO J*. 2011;30(17):3620-3634.
43. Kometani K, Yamada T, Sasaki Y, et al. CIN85 drives B cell responses by linking BCR signals to the canonical NF-kappaB pathway. *J Exp Med*. 2011;208(7):1447-1457.
44. Buchse T, Horras N, Lenfert E, et al. CIN85 interacting proteins in B cells-specific role for SHIP-1. *Mol Cell Proteomics*. 2011;10(10):M110.

Reduced carotid intima–media thickness in systemic lupus erythematosus patients treated with cyclosporine A

Kensuke Oryoji · Chikako Kiyohara · Takahiko Horiuchi · Hiroshi Tsukamoto · Hiroaki Niiro · Terufumi Shimoda · Koichi Akashi · Toshihiko Yanase

Received: 8 November 2012 / Accepted: 28 December 2012
© Japan College of Rheumatology 2013

Abstract

Background Patients with systemic lupus erythematosus (SLE) are at risk of atherosclerosis. An increased carotid intima–media thickness (IMT) is considered to be a marker of early atherosclerosis.

Objective To determine influential factors for increased carotid IMT in SLE patients.

Methods We evaluated the impact of conventional risk factors for atherosclerosis on carotid IMT in 427 healthy controls and of clinical factors on carotid IMT in 94 SLE patients. Carotid IMT was measured by using a newly developed computer-automated system. Unconditional logistic regression was used to assess the adjusted odds ratios (ORs) and 95 % confidence intervals (95 % CI).

Results Multivariate-adjusted mean carotid IMT (mm) was significantly reduced in SLE patients (0.51, 95 % CI = 0.36–0.66) compared to healthy controls (0.55, 95 % CI = 0.40–0.70) ($P = 0.003$). The SLE Disease Activity Index (SLEDAI) was associated with carotid IMT in a

dose-dependent manner ($P_{\text{trend}} = 0.041$). The current use of cyclosporine A (adjusted OR = 0.02, 95 % CI = 0.01–0.40, $P = 0.011$) and a history of steroid pulse therapy (adjusted OR = 0.01, 95 % CI = 0.01–0.25, $P = 0.006$) were significantly associated with a decreased risk of increased carotid IMT.

Conclusions Our findings suggest that the current use of cyclosporine A can protect against increased carotid IMT, leading to a decreased risk of arteriosclerosis. Future studies with a larger sample size need to confirm that this association holds longitudinally.

Keywords Cyclosporine A · Carotid intima–media thickness · Systemic lupus erythematosus · Risk factor

Introduction

Systemic lupus erythematosus (SLE) exhibits a bimodal pattern of mortality, where early deaths are caused by uncontrolled disease activity, while later deaths are mostly attributed to cardiovascular complications [1]. Subsequent follow-up studies have demonstrated that the incidence of coronary artery disease in women with SLE is five to nine times higher compared with the general population [2–4]. These data indicate that there is a strong association between SLE and cardiovascular diseases. As the main etiological cause of cardiovascular diseases can be attributed to atherosclerosis, the assessment of risk factors for atherosclerosis is important for the control of morbidity and mortality in SLE.

The status of atherosclerosis has been assessed by a number of surrogate markers. The structural markers include such measures as carotid intima–media thickness (IMT) and the presence of plaques, while functional

K. Oryoji · T. Horiuchi (✉) · H. Tsukamoto · H. Niiro · K. Akashi
Department of Medicine and Biosystemic Science,
Kyushu University Graduate School of Medical Sciences,
Fukuoka 812-8582, Japan
e-mail: horiuchi@intmed1.med.kyushu-u.ac.jp

C. Kiyohara
Department of Preventive Medicine, Kyushu University
Graduate School of Medical Sciences, Fukuoka 812-8582, Japan

T. Shimoda
Department of Clinical Research, National Fukuoka Hospital,
Fukuoka 811-1394, Japan

T. Yanase
Department of Endocrinology and Diabetes Mellitus, School
of Medicine, Fukuoka University, Fukuoka 814-0180, Japan

markers are for example pulse wave velocity and flow-mediated dilatation of arteries. Among the measures, most of longitudinal studies have demonstrated the usefulness of carotid IMT in predicting future vascular events including myocardial infarction and stroke, which was confirmed by a recent meta-analysis [5]. Carotid IMT evaluated by B-mode ultrasonography has become a simple and non-invasive measure for early atherosclerosis. However, carotid IMT has some difficulties in accuracy and reproducibility, because it is evaluated by the manual eye-measurement method, usually at only three sites each of the carotid arteries. To resolve these problems, a new computer-automated system using Intimascope[®] software was developed, which enabled the averaging approximately 250 points in 2 cm of carotid artery, therefore being highly useful in carotid IMT measurement [6, 7].

We here compared conventional risk factors for atherosclerosis, including carotid IMT measured by using the newly developed computer-aided system, in a case control study including 92 SLE patients and 184 healthy controls in a female Japanese population. In addition, we evaluated the impact of conventional factors for atherosclerosis on carotid IMT in 427 healthy controls (both sexes) and the impact of clinical status and treatment on carotid IMT in 92 SLE patients.

Patients and methods

Patients and controls

The 92 patients with SLE enrolled in the study were all women and fulfilled the American College of Rheumatology classification criteria for SLE, followed at the Department of Medicine and Biosystemic Science, Kyushu University, from 2007 to 2008. Controls (243 men and 184 women) were recruited from the Human Dry Dock Center, Wellness (Fukuoka, Japan), for a routine health evaluation in September, 2002. Blood samples were obtained from SLE patients and healthy controls in a fasting state. Serum concentrations of total cholesterol (T-chol), triglyceride, HDL cholesterol (HDL-chol), fasting blood sugar (FBS), glycosylated hemoglobin (HbA_{1c}) and high-sensitivity C-reactive protein (CRP) were measured. Serum concentrations of LDL cholesterol (LDL-chol) were calculated by the Friedewald formula [8]. The details of the control group were reported elsewhere [6]. Disease activity was measured by the SLE disease activity index (SLEDAI) [9] and damage by the Systemic Lupus International Collaborating Clinics/American College of Rheumatology Damage Index (SDI) [10]. Part of the data has been reported previously [6]. All individuals were Japanese. The study protocol was approved by our institutional review board, and all participants provided written informed consent.

Statistical analysis

Comparison of means and proportions between two groups was done by *t* test and χ^2 test, respectively. Among three groups, *P* values were calculated by analysis of covariance and were adjusted by use of the Bonferroni correction. The trend of association between clinical status and carotid IMT was assessed by a regression model assigning ordinal scores to the levels of the independent variable. Unconditional logistic regression was used to compute the odds ratios (ORs) and their 95 % confidence intervals (CIs) with adjustments for several covariates. A continuous variable was used for age, and the remaining covariates were treated as a categorical variable. Multicollinearity among all independent variables was evaluated by Pearson correlation. The covariates were basically categorized into three categories using tertiles in the controls as cutoff points. The distribution of CRP concentrations was skewed to the right, and natural logarithms of these values were used in the statistical analysis. The cumulative steroid dose was estimated using the equation $1/2$ (maximum steroid dose + current steroid dose) \times (the duration of administration). Body mass index (BMI, kg/m²) was classified into three groups (<19.8, 19.9–21.4 and >21.5); FBS (mg/dl) into three groups (<86, 87–92, >93); carotid IMT (mm) into three groups (<0.50, 0.51–0.57 and >0.58); T-chol (mmol/l) into three groups (<190, 191–217 and >218); DBP (mmHg) into three groups (<57, 58–65 and >66) and CRP (mg/dl) into three groups (<0.016, 0.017–0.045 and >0.046). The estimated steroid dose (g) was categorized into two groups (<127.75 and \geq 127.75); SLEDAI into three groups (0–2, 3–5 and \geq 6) and SDI into two groups (0–1 and \geq 2). When multicollinearity exists, the standard errors for the coefficients tend to be very large, inflating the standard errors of the regression coefficients, which in turn become unreliable. Triglycerides, HDL-chol and LDL-chol were significantly related to and suspected to have multicollinearity with total cholesterol [$r = 0.35$ ($P < 0.001$), $r = 0.12$ ($P = 0.017$) and $r = 0.81$ ($P < 0.001$), respectively] in healthy controls. HbA_{1c} was excluded from the multivariate analysis because of the collinearity between FBS and HbA_{1c} ($r = 0.83$, $P < 0.001$). Similarly, we did not include SBP in multivariate models because of collinearity between DBP and SBP ($r = 0.84$, $P < 0.001$). We also excluded body fat (%) because of collinearity between BMI and body fat ($r = 1.00$, $P < 0.001$). Lastly, disease duration was excluded from the multivariate analysis because of high correlation with age ($r = 0.60$, $P < 0.001$).

All statistical analyses were performed using the computer program STATA version 12.1 (STATA Corp., College Station, TX, USA). All *P* values were two-sided, with those less than 0.05 considered statistically significant.

Results

Table 1 shows a comparison of the risk factors for atherosclerosis between SLE patients and healthy controls in a female Japanese population. The mean age of SLE patients (43.7, 95 % CI = 41.0–46.4) was not significantly different from that of controls (45.7, 95 % CI = 44.5–47.0; data not shown). Female SLE patients (20.0, 95 % CI = 15.1–25.0) showed significantly lower BMIs than female healthy controls (21.3, 95 % CI = 16.4–26.2; $P = 0.004$). DBP (mmHg) ($P < 0.0001$) was significantly higher in SLE patients (75.5, 95 % CI = 58.4–92.6) than in healthy controls (64.0, 95 % CI = 47.0–80.9), while

Table 1 Comparison of risk factors for atherosclerosis between SLE patients and healthy controls in a female Japanese population

	SLE patients (<i>n</i> = 92)	Female controls (<i>n</i> = 184)	<i>P</i>
BMI (kg/m²)			
Crude	21.1 (20.5–21.6)	21.1 (20.7–21.5)	0.874
Age-adjusted	21.1 (20.6–21.7)	21.1 (20.7–21.5)	0.876
Multivariate-adjusted ^a	20.0 (15.1–25.0)	21.3 (16.4–26.2)	0.004
T-chol (mmol/l)			
Crude	197 (190–205)	205 (200–210)	0.105
Age-adjusted	199 (193–206)	204 (199–209)	0.267
Multivariate-adjusted ^a	195 (134–257)	206 (144–267)	0.064
FBS (mg/dl)			
Crude	89.8 (85.5–94.0)	91.9 (89.4–94.3)	0.397
Age-adjusted	89.9 (85.7–94.1)	91.7 (89.3–94.1)	0.467
Multivariate-adjusted ^a	88.1 (55.6–121)	92.6 (60.3–125)	0.119
CRP (mg/dl)^b			
Crude	0.04 (0.03–0.06)	0.02 (0.02–0.03)	0.004
Age-adjusted	0.05 (0.03–0.06)	0.02 (0.02–0.03)	<0.0001
Multivariate-adjusted ^a	0.04 (0.03–0.05)	0.02 (0.02–0.03)	0.059
DBP (mmHg)			
Crude	74.5 (72.6–76.4)	64.0 (62.6–65.3)	<0.0001
Age-adjusted	74.9 (73.0–76.7)	63.8 (62.5–65.1)	<0.0001
Multivariate-adjusted ^a	75.5 (58.4–92.6)	64.0 (47.0–80.9)	<0.0001
Carotid IMT (mm)			
Crude	0.52 (0.50–0.54)	0.55 (0.54–0.56)	0.007
Age-adjusted	0.52 (0.51–0.54)	0.55 (0.53–0.56)	0.027
Multivariate-adjusted ^a	0.51 (0.36–0.66)	0.55 (0.40–0.70)	0.003

BMI body mass index, *T-chol* total cholesterol, *FBS* fasting blood sugar, *CRP* high-sensitivity C-reactive protein, *IMT* intima-media thickness

^a Adjusted for age, FBS, BMI, IMT, T-chol, DBP and CRP

^b Geometric mean

carotid IMT ($P = 0.003$) was significantly lower in SLE patients (0.51 mm, 95 % CI = 0.36–0.66) compared to healthy controls (0.55 mm, 95 % CI = 0.40–0.70). SLE patients showed marginally lower T-chol ($P = 0.064$) and marginally higher CRP ($P = 0.059$) than healthy controls.

Comparison of selected characteristics between healthy subjects in the highest quartile of carotid IMT (≥ 0.63 mm) and those in the remaining three quartiles (< 0.63 mm) is shown in Table 2. Subjects in the highest quartile showed higher age ($P < 0.001$), prevalence of male sex ($P = 0.002$), and levels of FBS ($P = 0.001$), T-chol ($P = 0.005$), LDL-chol ($P < 0.001$), HbA_{1c} ($P < 0.001$), CRP ($P = 0.001$), BMI ($P < 0.001$), DBP ($P < 0.001$) and SBP ($P < 0.001$) than those in the remaining three quartiles. In contrast, the HDL-chol level was significantly lower in subjects in the highest quartile than in those in the remaining three quartiles ($P = 0.005$).

Detailed characteristics of our SLE patients including the number of each treatment, average and cumulative steroid dose, and disease duration are demonstrated in Table 3. Table 4 shows the association between disease activity or disease damage and carotid IMT in SLE patients. After adjustment for age, FBS, BMI, T-chol, DBP

Table 2 Comparison of selected characteristics between healthy subjects in the highest quartile of carotid IMT and those in the remaining three quartiles

	Highest quartile ^a (<i>n</i> = 99)	Remaining three quartiles (<i>n</i> = 328)	<i>P</i>
Age (years)	53.1 (51.4–54.7)	45.0 (44.1–45.9)	<0.001
Male sex, <i>n</i> (%)	70 (70.7)	173 (52.7)	0.002
Prevalence of smokers, <i>n</i> (%) ^b	29 (36.3)	76 (27.4)	0.128
Prevalence of drinkers, <i>n</i> (%) ^b	74 (74.8)	235 (71.9)	0.574
FBS (mg/dl)	102 (94.7–107)	94.8 (92.9–96.7)	0.001
T-chol (mmol/l)	213 (206–221)	203 (199–206)	0.005
HDL-chol (mmol/l)	54.6 (51.9–57.3)	59.3 (57.7–60.9)	0.005
LDL-chol (mmol/l)	133 (126–139)	120 (117–123)	<0.001
Triglycerides (mmol/l)	131 (112–151)	119 (107–130)	0.296
HbA _{1c} (%)	5.14 (4.96–5.33)	4.82 (4.76–4.88)	<0.001
CRP (mg/dl) ^c	0.04 (0.04–0.05)	0.03 (0.03–0.03)	0.001
BMI (kg/m ²)	24.2 (23.5–24.9)	22.2 (21.9–22.6)	<0.001
Body fat (%)	25.2 (24.1–26.3)	24.0 (23.5–24.6)	0.057
DBP (mmHg)	77.1 (68.9–73.4)	66.9 (65.8–68.0)	<0.001
SBP (mmHg)	119 (115–122)	112 (110–113)	<0.001

IMT intima-media thickness, *FBS* fasting blood sugar, *T-chol* total cholesterol, *HbA_{1c}* glycosylated hemoglobin, *CRP* high-sensitivity C-reactive protein, *BMI* body mass index

^a Mean IMT ≥ 0.63 mm

^b Several observations with missing values

^c Geometric mean

and CRP, SLE patients with the highest SLEDAI (6+) showed a significantly higher carotid IMT [0.57 mm (95 % CI = 0.44–0.68) vs. 0.48 mm (95 % CI = 0.36–0.59)] than patients with the lowest SLEDAI (0–2) ($P = 0.027$, ANCOVA followed by the Bonferroni test). SLEDAI was associated with carotid IMT in a dose-dependent manner ($P_{\text{trend}} = 0.041$). SDI was not associated with carotid IMT, however.

The ORs of increased carotid IMT (>0.5 mm, above median) in relation to treatment for SLE are shown in Table 5. Multivariate-adjusted OR of increased carotid IMT for current users of cyclosporine A versus nonuser of

cyclosporine A was 0.02 (95 % CI = 0.01–0.40, $P = 0.011$). Similarly, the patients who had a history of steroid pulse therapy revealed a reduced risk of increased carotid IMT (OR = 0.01, 95 % CI = 0.01–0.25, $P = 0.006$). In contrast, current use of NSAIDs was marginally associated with an increased risk of increased carotid IMT (OR = 0.56, 95 % CI = 0.97–32.3, $P = 0.054$). The remaining treatment factors were not associated with the risk of increased carotid IMT.

Discussion

The mechanism of accelerated atherosclerosis in SLE is unclear. It is likely to be due to conventional risk factors, factors related to the disease itself and/or treatment factors for SLE. In this study, female SLE patients showed significantly lower BMIs than female healthy controls ($P = 0.004$). Based on data from the National Health and Nutrition Survey in Japan in 2008, the mean BMI among women in their 40s has been reported to be 22.2 [11]. BMI was lower in our healthy controls than in the female general population. Although SLE patients have a higher prevalence of obesity [12], the mean BMI was similar between SLE patients and healthy controls [12, 13]. Although little is known about the effects of obesity in SLE patients, SLE patients were instructed to lose weight because they are at risk of atherosclerosis. As a result, BMI can be decreased in SLE patients. SLE patients showed marginally lower T-chol ($P = 0.064$). This was just as valid for T-chol. Multivariate-adjusted mean of CRP was marginally higher in SLE patients than in healthy controls ($P = 0.064$). It has been reported that modest CRP elevation is common in SLE patients [14].

Table 3 Detailed characteristics of SLE patients

Variable	Mean (range) or <i>n</i> (%)
Age (years)	43.74 (18–77)
Age at diagnosis (years)	29.93 (10–68)
Disease duration (years)	14.12 (0–35)
SLEDAI	4.11 (0–16)
SDI	1.08 (0–4)
Cumulative steroid use (g)	128.52 (0–347.48)
Past user of cyclosporine A	18 (19.57)
Current user of cyclosporine A	13 (14.13)
Past user of cyclophosphamide	15 (16.30)
Current user of cyclophosphamide	0 (0.00)
Current user of tacrolimus	8 (8.70)
Current user of statins	26 (28.26)
Current user of NSAIDs	36 (39.13)
Current user of warfarin	15 (16.30)
Current user of CaB	19 (20.65)
Current user of ARBs	23 (25.00)
Having a history of steroid pulse therapy	20 (21.74)

Table 4 Association between clinical status and carotid IMT

Clinical status	<i>n</i>	Mean carotid IMT (95 % CI), mm			
		Crude	<i>P</i>	Adjusted ^a	<i>P</i>
SLEDAI					
0–2	44	0.49 (0.47–0.52)	0.025	0.48 (0.36–0.59)	0.027
3–5	21	0.52 (0.50–0.54)		0.52 (0.41–0.64)	
6+	27	0.55 (0.52–0.58)		0.57 (0.44–0.68)	
		$P_{\text{trend}} < 0.0001$		$P_{\text{trend}} = 0.041$	
SDI					
0–1	64	0.51 (0.48–0.53)		0.51 (0.37–0.65)	
2+	28	0.54 (0.51–0.57)	0.070	0.51 (0.37–0.65)	0.719

CI confidence interval, IMT intima–media thickness

^a Adjusted for age, FBS, BMI, T-chol, DBP and CRP

Table 5 Multivariate-adjusted ORs (95 % CI) of increased carotid IMT (>0.5 mm) in relation to treatment for SLE

Treatment factor	OR (95 % CI)			
	Crude	<i>P</i>	Adjusted ^a	<i>P</i>
Past use of cyclosporine A				
Positive vs. negative	0.46 (0.16–1.32)	0.147	1.26 (0.19–8.15)	0.811
Current use of cyclosporine A				
Positive vs. negative	0.12 (0.02–0.57)	0.008	0.02 (0.01–0.40)	0.011
Past use of cyclophosphamide				
Positive vs. negative	1.31 (0.43–4.06)	0.632	0.21 (0.02–2.63)	0.226
Current use of tacrolimus				
Positive vs. negative	0.83 (0.19–3.53)	0.796	0.69 (0.07–7.22)	0.759
Cumulative steroid use (g)				
>127.75 vs. 0–127.75	2.32 (1.00–5.39)	0.050	2.44 (0.46–12.9)	0.295
Current use of statins				
Positive vs. negative	1.89 (0.74–4.84)	0.185	0.34 (0.04–2.89)	0.321
Current use of NSAIDs				
Positive vs. negative	1.30 (0.56–3.03)	0.539	5.60 (0.97–32.3)	0.054
Current use of warfarin				
Positive vs. negative	0.69 (0.23–2.10)	0.515	0.57 (0.06–4.95)	0.607
Current use of CaB				
Positive vs. negative	2.88 (0.94–8.82)	0.064	1.40 (0.23–8.44)	0.530
Current use of ARBs				
Positive vs. negative	3.09 (1.09–8.77)	0.034	2.04 (0.22–18.9)	0.720
History of steroid pulse therapy				
Positive vs. negative	0.27 (0.09–0.79)	0.017	0.01 (0.01–0.25)	0.006

OR odds ratio, CI confidence interval, IMT intima–media thickness, NSAIDs non-steroidal anti-inflammatory drugs, CaB calcium blocker, AB angiotensin receptor blockers

^a Adjusted for age, DBP, BMI, T-chol, CRP and SLEDAI

It is generally accepted that CRP levels less than 0.3 mg/dl (range 0–1 mg/l) are considered normal [14, 15]. Therefore, mean CRP levels of SLE patients remain within the normal range. DBP was significantly higher in SLE patients than in healthy controls ($P < 0.0001$). Based on data from the National Health and Nutrition Survey in Japan in (2008), the mean DBP among women in their 40s has been reported to be 76 mmHg [11]. DBP was somewhat lower in our SLE patients (74.5 mmHg) than in the general female population (76 mmHg). As the means of BMI, T-chol, FBS and DBP were lower in our female

controls than in the female general population, our controls (health checkup examinees) are possibly healthier than the general population. Health check examinees are concerned with the maintenance and promotion of their health (self-selection bias). Unexpectedly, carotid IMT was significantly lower in SLE patients compared to healthy controls ($P = 0.003$). As discussed previously, the difference in carotid IMT may become more exaggerated when our SLE patients and female general population are compared. Roman et al. [16] also reported that carotid IMT was significantly less in SLE patients than controls. Some studies reported that SLE patients had a greater carotid IMT than population controls [17–20], while other studies found no significant difference between the two groups [21–25]. A considerable number of factors such as the carotid IMT measurement method, study population characteristics and disease activity may explain this unanticipated discrepant result. In this study, we used a newly developed computer-automated system that provided more accurate IMT data compared to the conventional manual eye-measurement method. Male sex, FBS, HbA_{1c}, T-chol, LDL-chol, triglycerides, CRP, BMI DBP and SBP were significantly related with carotid IMT in 427 healthy controls (Table 2). Similar results have been reported in many studies [26–30], but most of these were reported in populations that included patients with coronary artery disease, hypercholesterolemia, cerebrovascular disease, diabetes mellitus and hypertension. As shown in Table 4, SLEDAI was positively associated with carotid IMT. Carotid IMT is a simple and noninvasive method and is increasingly used as a surrogate marker of atherosclerosis [5]. Atherosclerosis is characterized by infiltration of the intima by activated macrophages and T cells, and it is thus considered to be caused by inflammatory processes [31]. Vasculitis is a common feature of SLE. Deposition of circulating immune complexes in SLE is supposed to lead to the leukocyte adhesion and activation, production of cytokine and other inflammatory mediators [32]. It is therefore conceivable that carotid IMT was increased in SLE patients with higher disease activity, namely with higher SLEDAI. In contrast, accumulated damage in SLE (SDI) was not associated with carotid IMT. Carotid IMT may reflect the current, and not the past, inflammatory status in the vessels.

As shown in Table 5, a history of steroid pulse therapy was associated with decreased carotid IMT. As steroid pulse therapy is given to SLE patients with the most severe disease activity, intensive care and swift disease control of SLE might overcome the possible pro-atherosclerotic effect of prednisolone when the pro-atherosclerotic effect of SLE disease activity is considered. In addition, cumulative steroid use did not have any association with the carotid IMT in our SLE patients. Increased cumulative

dosage of steroid by a long-term low-dose prednisolone therapy may not be a risk factor for atherosclerosis in SLE, because a prospective study showed that a low-dose prednisolone therapy does not influence atherosclerosis, as determined by carotid IMT in rheumatoid arthritis patients for at least 2 years [33]. Current use of cyclosporine A was significantly associated with decreased carotid IMT (Table 5). Cyclosporine A blocks the phosphatase activity of calcineurin, an essential component of the T cell activation pathway, and is thus considered to be a strong inhibitor of the immune system, most notably of T cells [34]. Tacrolimus was not associated with carotid IMT in our cases, which may not be surprising. Although cyclosporine A and tacrolimus share a common mechanism of calcineurin inhibition, there have been reported differential effects on the molecules other than calcineurin [35]. In fact, clinical effects and adverse events of these two calcineurin inhibitors are not similar, as evidenced in the previous 2 decades of data on organ transplantation [35]. As the number of patients on tacrolimus is small ($n = 8$), further study with a larger sample size is needed before reaching a conclusion. A protective effect of cyclosporine A use against carotid IMT has also been reported by others [36]. Cyclosporine A might be added to the treatment of choice from the standpoint view of reduction of carotid IMT and the resultant prevention of atherosclerosis in SLE.

In conclusion, multivariate-adjusted mean carotid IMT was significantly reduced in SLE patients compared to healthy controls ($P = 0.003$). The current use of cyclosporine A ($P = 0.011$) and a history of steroid pulse therapy ($P = 0.006$) were significantly associated with decreased carotid IMT, while current use of NSAIDs ($P = 0.054$) was marginally associated with increased carotid IMT. Advances in medical therapy and a better understanding of SLE have contributed to a dramatic improvement in the long-term survival of patients.

Acknowledgments This work was supported in part by grants from Ministry of Education, Culture, Sports, Science and Technology, Japan. We thank Ms Chitose Matsuzaki for her excellent technical assistance.

Conflict of interest None.

References

- Urowitz MB, Bookman AA, Koehler BE, Gordon DA, Smythe HA, Ogryzlo MA. The bimodal mortality pattern of systemic lupus erythematosus. *Am J Med.* 1976;60:221–5.
- Trager J, Ward MM. Mortality and causes of death in systemic lupus erythematosus. *Curr Opin Rheumatol.* 2001;13:345–51.
- Esdaille JM, Abrahamowicz M, Grodzicky T, et al. Traditional Framingham risk factors fail to fully account for accelerated atherosclerosis in systemic lupus erythematosus. *Arthritis Rheum.* 2001;44:2331–7.
- Manzi S, Urbach AH, McCune AB, et al. Systemic lupus erythematosus in a boy with chronic granulomatous disease: case report and review of the literature. *Arthritis Rheum.* 1991;34:101–5.
- Lorenz MW, Markus HS, Bots ML, Rosvall M, Sitzer M. Prediction of clinical cardiovascular events with carotid intima-media thickness: a systematic review and meta-analysis. *Circulation.* 2007;115:459–67.
- Yanase T, Nasu S, Mukuta Y, et al. Evaluation of a new carotid intima-media thickness measurement by B-mode ultrasonography using an innovative measurement software, intimascope. *Am J Hypertens.* 2006;19:1206–12.
- Nohara R, Daida H, Hata M, et al. Effect of intensive lipid-lowering therapy with rosuvastatin on progression of carotid intima-media thickness in Japanese patients: justification for Atherosclerosis Regression Treatment (JART) study. *Circ J.* 2012;76:221–9.
- Friedewald WT, Levy RI, Fredrickson DS. Estimation of the concentration of low-density lipoprotein cholesterol in plasma, without use of the preparative ultracentrifuge. *Clin Chem.* 1972;18:499–502.
- Bombardier C, Gladman DD, Urowitz MB, Caron D, Chang CH. Derivation of the SLEDAI. A disease activity index for lupus patients. The Committee on Prognosis Studies in SLE. *Arthritis Rheum.* 1992;35:630–40.
- Gladman D, Ginzler E, Goldsmith C, et al. The development and initial validation of the Systemic Lupus International Collaborating Clinics/American College of Rheumatology damage index for systemic lupus erythematosus. *Arthritis Rheum.* 1996;39:363–9.
- MHLW. 2008 [updated 2008; cited]. <http://www.mhlw.go.jp/bunya/kenkou/eiyou/h20-houkoku.html>.
- Chaiamnuy S, Bertoli AM, Fernandez M, et al. The impact of increased body mass index on systemic lupus erythematosus: data from LUMINA, a multiethnic cohort (LUMINA XLVI) [corrected]. *J Clin Rheumatol.* 2007;13:128–33.
- Colombo BM, Murdaca G, Ciprandi G, Sormani MP. Body mass index in Th1 and Th2 diseases. *Immunol Lett.* 2008;117:119–20.
- Gaitonde S, Samols D, Kushner I. C-reactive protein and systemic lupus erythematosus. *Arthritis Rheum.* 2008;59:1814–20.
- Roy S, Tan KT. Pyrexia and normal C-reactive protein (CRP) in patients with systemic lupus erythematosus: always consider the possibility of infection in febrile patients with systemic lupus erythematosus regardless of CRP levels. *Rheumatology (Oxford).* 2001;40:349–50.
- Roman MJ, Shanker BA, Davis A, et al. Prevalence and correlates of accelerated atherosclerosis in systemic lupus erythematosus. *N Engl J Med.* 2003;349:2399–406.
- Svenungsson E, Jensen-Urstad K, Heimburger M, et al. Risk factors for cardiovascular disease in systemic lupus erythematosus. *Circulation.* 2001;104:1887–93.
- Ugurlu S, Seyahi E, Cetinkaya F, Ozbakir F, Balci H, Ozdogan H. Intima-media thickening in patients with familial Mediterranean fever. *Rheumatology (Oxford).* 2009;48:911–5.
- Zhang CY, Lu LJ, Li FH, et al. Evaluation of risk factors that contribute to high prevalence of premature atherosclerosis in Chinese premenopausal systemic lupus erythematosus patients. *J Clin Rheumatol.* 2009;15:111–6.
- Bicakcigil M, Tasan D, Tasdelen N, Mutlu N, Yavuz S. Role of fibrinolytic parameters and plasminogen activator inhibitor 1 (PAI-1) promoter polymorphism on premature atherosclerosis in SLE patients. *Lupus.* 2011;20:1063–71.
- Jimenez S, Garcia-Criado MA, Tassies D, et al. Preclinical vascular disease in systemic lupus erythematosus and primary antiphospholipid syndrome. *Rheumatology (Oxford).* 2005;44:756–61.

22. Sari I, Karaoglu O, Can G, et al. Early ultrasonographic markers of atherosclerosis in patients with familial Mediterranean fever. *Clin Rheumatol*. 2007;26:1467–73.
23. Thompson T, Sutton-Tyrrell K, Wildman RP, et al. Progression of carotid intima–media thickness and plaque in women with systemic lupus erythematosus. *Arthritis Rheum*. 2008;58:835–42.
24. Rossi M, Mosca M, Tani C, Franzoni F, Santoro G, Bombardieri S. Integrated backscatter analysis of carotid intima–media complex in patients with systemic lupus erythematosus. *Clin Rheumatol*. 2008;27:1485–8.
25. Santos MJ, Pedro LM, Canhao H, et al. Hemorheological parameters are related to subclinical atherosclerosis in systemic lupus erythematosus and rheumatoid arthritis patients. *Atherosclerosis*. 2011;219:821–6.
26. Sharrett AR, Patsch W, Sorlie PD, Heiss G, Bond MG, Davis CE. Associations of lipoprotein cholesterol, apolipoproteins A-I and B, and triglycerides with carotid atherosclerosis and coronary heart disease. The Atherosclerosis Risk in Communities (ARIC) Study. *Arterioscler Thromb*. 1994;14:1098–104.
27. Crouse JR, Goldbourt U, Evans G, et al. Risk factors and segment-specific carotid arterial enlargement in the Atherosclerosis Risk in Communities (ARIC) cohort. *Stroke*. 1996;27:69–75.
28. Tonstad S, Joakimsen O, Stensland-Bugge E, et al. Risk factors related to carotid intima–media thickness and plaque in children with familial hypercholesterolemia and control subjects. *Arterioscler Thromb Vasc Biol*. 1996;16:984–91.
29. Folsom AR, Pankow JS, Williams RR, Evans GW, Province MA, Eckfeldt JH. Fibrinogen, plasminogen activator inhibitor-1, and carotid intima–media wall thickness in the NHLBI Family Heart Study. *Thromb Haemost*. 1998;79:400–4.
30. Davis PH, Dawson JD, Riley WA, Lauer RM. Carotid intimal-medial thickness is related to cardiovascular risk factors measured from childhood through middle age: the Muscatine Study. *Circulation*. 2001;104:2815–9.
31. Ross R. Atherosclerosis—an inflammatory disease. *N Engl J Med*. 1999;340:115–26.
32. Kallenberg CG, Heeringa P. Pathogenesis of vasculitis. *Lupus*. 1998;7:280–4.
33. Doria A, Shoenfeld Y, Wu R, et al. Risk factors for subclinical atherosclerosis in a prospective cohort of patients with systemic lupus erythematosus. *Ann Rheum Dis*. 2003;62:1071–7.
34. Schreiber SL, Crabtree GR. The mechanism of action of cyclosporin A and FK506. *Immunol Today*. 1992;13:136–42.
35. Maes BD, Vanrenterghem YF. Cyclosporine: advantages versus disadvantages vis-a-vis tacrolimus. *Transpl Proc*. 2004;36:40S–9S.
36. Sazliyana S, Mohd Shahrir MS, Kong CT, Tan HJ, Hamidon BB, Azmi MT. Implications of immunosuppressive agents in cardiovascular risks and carotid intima media thickness among lupus nephritis patients. *Lupus*. 2011;20:1260–6.

Prevalence and risk factors of vertebral fracture in female Japanese patients with systemic lupus erythematosus

Makio Furukawa · Chikako Kiyohara · Takahiko Horiuchi · Hiroshi Tsukamoto · Hiroki Mitoma · Yasutaka Kimoto · Ayumi Uchino · Misato Nakagawa · Kensuke Oryoji · Terufumi Shimoda · Mine Harada · Koichi Akashi

Received: 8 March 2012 / Accepted: 30 July 2012
© Japan College of Rheumatology 2012

Abstract

Objective We examined the prevalence and risk factors of vertebral fracture in female Japanese patients with systemic lupus erythematosus (SLE).

Methods We performed lateral radiographs of the thoracic and lumbar spine and bone mineral density (BMD) measurements and collected demographic, lifestyle, clinical, and treatment characteristics of 52 SLE patients. Vertebral fractures were defined as a >20 % reduction of vertebral body height. Odds ratios (ORs) and their 95 % confidence intervals (CIs) were computed to assess the strength of associations between vertebral fractures and selected factors among SLE patients.

Results At least one vertebral fracture was detected in 50 % of SLE patients. A history of previous bone fracture was significantly associated with an increased risk of vertebral fractures among SLE patients (adjusted OR = 14.8, 95 % CI = 1.62–134; $P = 0.017$). Daily use of tea or

coffee was marginally associated with a decreased risk of vertebral fractures among SLE patients (adjusted OR = 0.11, 95 % CI = 0.01–1.01; $P = 0.051$).

Conclusion The high prevalence of vertebral fracture in SLE patients (50 %) indicates that we need to assess the lateral spine radiograph in more female Japanese SLE patients regardless of BMD and use of corticosteroids, although additional studies are warranted to confirm the findings suggested in this study.

Keywords Vertebral fracture · Systemic lupus erythematosus · Japanese

Introduction

Due to improved treatments, the survival of patients with systemic lupus erythematosus (SLE) has improved dramatically over the last few decades [1], resulting in long-term morbidity with osteoporosis and osteoporotic fractures. Patients with SLE are thought to be at risk of osteoporosis because of factors such as inflammation, premature menopause, renal involvement, proinflammatory cytokine production [2], estrogen reduction, exposure to corticosteroids (CS), and vitamin D deficiency [3]. Vertebral fractures are a complication of osteoporosis. Several studies demonstrate a high prevalence (25–46 %) of low bone mineral density (BMD) in female patients with SLE [4–9] in comparison with the general population. Low BMD is a risk factor of vertebral fractures. Recent studies, however, show that vertebral compression fractures are common in SLE patients with normal BMD, indicating alternative mechanisms of compression fractures [10]. The prevalence of vertebral fractures in Japanese SLE patients remains unclear. There are very few published data on the

M. Furukawa · T. Horiuchi · H. Tsukamoto · H. Mitoma · Y. Kimoto · A. Uchino · M. Nakagawa · K. Oryoji · K. Akashi
Department of Medicine and Biosystemic Science, Graduate School of Medical Sciences, Kyushu University, 3-1-1 Maidashi, Higashi-ku, Fukuoka 812-8582, Japan

C. Kiyohara (✉)
Department of Preventive Medicine, Graduate School of Medical Sciences, Kyushu University, 3-1-1 Maidashi, Higashi-ku, Fukuoka 812-8582, Japan
e-mail: chikako@phealth.med.kyushu-u.ac.jp

T. Shimoda
Department of Clinical Research, Fukuoka National Hospital, 4-39-1 Yakatabaru, Minami-ku, Fukuoka 811-1394, Japan

M. Harada
Omuta National Hospital, 1044-1 Tachibana, Omuta 837-0911, Japan

prevalence and the risk factors of vertebral fractures in Caucasian SLE patients [10–13]. The majority of SLE patients use CS, which induce bone loss and increase fracture risk. Ramsay–Goldman et al. [14] described a fivefold increase in fracture rates in US women with SLE. CS treatment affects trabecular bone preferentially; therefore, vertebrae, which consist mostly of trabecular bone, are major targets of the deleterious effects of glucocorticoids [15, 16].

The importance of identifying vertebral fractures in SLE patients is illustrated by the observed association between vertebral deformities and reduced quality of life in postmenopausal women with osteoporosis [17], as well as increased risk of future vertebral and nonvertebral fractures and mortality rates in the general population [18]. To investigate the prevalence of vertebral fractures and, if possible, risks or preventive factors associated with vertebral fractures in female Japanese patients with SLE, we performed radiographs of the thoracic and lumbar spine in 52 such women and collected demographic, lifestyle, clinical, and treatment data.

Patients and methods

Patients

Fifty-two consecutive female Japanese patients with SLE were evaluated. All patients regularly attended the rheumatology clinic of Kyushu University Hospital. All patients fulfilled the 1997 American College of Rheumatology (ACR) revised criteria for SLE classification [19] and were informed of the objectives of the study and provided written informed consent for their participation. The study was approved by the ethical review board of Kyushu University Hospital.

Data collection and measurement

All measurements were performed from January to August 2006. Data were collected by questionnaire survey. Demographic and lifestyle data were obtained regarding age, BMI, and menstrual (presence of regular menstruation and menopause) and obstetric history (number of deliveries). In addition, we inquired about smoking; alcohol intake; exercise; going out; intake of milk, dairy products, fish, small fish, soybean products, coffee, tea, and Japanese green tea; use of sunscreen; and sleeping habits (bed or Japanese futon). Clinical data were assessed for disease duration, lupus nephritis (presence of persistent proteinuria of >0.5 g/24 h or cellular casts), photosensitivity, osteoporosis, bone and vertebral fractures, diabetes mellitus, hyperlipidemia, aseptic necrosis of the femoral bone, and

family history of osteoporosis or femoral neck (FN) fracture. We used the questionnaire to obtain information regarding family history. Laboratory data were obtained including complete blood count (CBC), urinary sediment, erythrocyte sedimentation rate (ESR), C-reactive protein (CRP), SCr (SCr), urinary creatinine (UCr), urinary protein (UP), serum bone-specific alkaline phosphatase (BAP), type I collagen cross-linked N-telopeptide (NTx), 25-hydroxy vitamin D, anti-double-stranded DNA (anti-dsDNA) antibodies, and complement components. We calculated creatinine clearance (CrCl) from SCr using the Cockcroft and Gault equation [20] and used UP/UCr to calculate uUP excretion per day [21]. A high titer of NTx was defined as a serum level >16.5 nmol BCE/l during premenopause and >24.0 nmol BCE/l during postmenopause, whereas low BAP titer was defined as a serum level <7.9 U/l based on the laboratory reference value. Disease activity was scored using the Systemic Lupus Erythematosus Disease Activity Index (SLEDAI) [22] by the attending physicians.

We performed BMD measurements of the lumbar spine (LS) (L2–L4) and hip (total hip: FN, trochanter, and intertrochanter), and lumbar spine and hip T-scores were reported. Measurements were performed using the same dual-energy X-ray absorptiometry (DEXA) equipment (model QDR-4500A; Hologic) by trained technicians. Hip measurement was not performed in four patients because of bilateral hip replacements. We used the standard definitions of osteoporosis [T score <-2.5 standard deviations (SD)] and osteopenia (-2.5 SD $<$ T score $<$ -1 SD). BMD with a T score <-1 SD was defined as low.

A history of CS and other immunosuppressant use was also obtained. We investigated past and current use of CS, duration of use in years, maximal dosage taken orally, current prednisone use, and past intravenous (IV) methylprednisolone use. In addition, we investigated past and current use of cyclosporin, methotrexate, cyclophosphamide, azathioprine, mizoribine, mycophenolate mofetil (MMF), rituximab, and IV administration of cyclophosphamide. We also inquired about current use of major or minor tranquilizers, antispasmodics, vitamin D supplements, hormone replacement therapy (HRT), vitamin K₂ supplements, warfarin, bisphosphonates (alendronates or risedronates), calcium supplements, contraceptive and vitamin C supplements orally, drugs prescribed in other hospitals, and supplements.

Assessment of vertebral deformities

We performed lateral radiographs of the thoracic and lumbar spine (Th4–L4) using the same equipment by trained technicians. Radiographs were scored by the same physician using a standardized semiquantitative method by

Genant et al. [23]. In this method, vertebrae are evaluated as follows: grade 0 normal, grade 1 20–25 % reduction in height, grade 2 25–40 % reduction in height, and grade 3 >40 % reduction in height. Vertebral deformities were scored according to the method of Genant et al. [23]; fractures were defined as a >20 % reduction of vertebral body height.

Statistical analysis

We first examined all variables found to have an association with vertebral fractures by univariate tests. Analysis of categorical (dichotomous) variables included frequency distributions, proportions, and statistical comparisons using Pearson's tests. We used the Student *t* test for analysis of continuous variables. Predictor variables with a level of significance $\leq 10\%$ ($P = 0.10$) for univariate tests were included as candidate predictors (risk factors) in the multivariable logistic regression model. Logistic regression analysis was used to obtain crude odds ratios (ORs) for the risk of vertebral fractures and the corresponding 95 % confidence intervals (95 % CIs), with adjustments for potential confounders. A *P* value ≤ 0.05 (two-sided) was considered statistically significant. All calculations were performed using STATA Version 8.2 (Stata Corporation, College Station, TX, USA) software.

Results

Measures of vertebral fracture

Assessment of vertebral deformities is shown in Table 1. Thoracic or lumbar spine vertebral deformities were observed in half (26/52) of SLE patients. At least 2 vertebral deformities were observed in 13 (25 %) SLE patients. We

Table 1 Assessment of vertebral deformity among SLE patients

Measures	Number (%)
Number of vertebral deformities	
0	26 (50)
1	13 (25)
>2	13 (25)
Severity of 46 vertebral deformities ($n = 26$)	
Grade 1 (20–25 % reduction of height)	36 (78.3)
Grade 2 (25–40 % reduction of height)	9 (19.6)
Grade 3 (>40 % reduction of height)	1 (2.2)
Distribution of 46 vertebral deformities ($n = 26$)	
Thoracic spine	34 (73.9)
Lumbar spine	12 (26.1)

detected a total of 46 deformities in 26 SLE patients. Of all vertebral deformities, 73.9 % were located in the thoracic spine and 26.1 % in the lumbar spine. In addition, 21.8 % of all vertebral deformities were grade 2 or higher.

Characteristics of study patients

Table 2 shows the characteristics of patients in the study. Mean age (SD) was 45.2 (13.8) years, and 37.3 % were postmenopausal. Mean body mass index (BMI) was 22.1 (3.7), mean disease duration (SD) was 17.1 (8.6) years, and mean SLEDAI (SD) was 7.2 (6.0). Twenty-four (52.2 %) patients had renal involvement and fifty (96.2 %) had a history of corticosteroid use. Forty-eight (92.3 %) were currently using CS, with a mean daily dose of 8.4 mg. As for osteoporosis treatments, vitamin D was currently used in 61.5 % and bisphosphonates in 40.4 %.

Comparison of demographic, lifestyle, clinical, and treatment factors between SLE patients with and without vertebral fractures

As shown in Table 2, the average age of SLE patients with vertebral deformities (50.0 years) was older than those without (40.3 years) ($P = 0.01$). Postmenopausal status was more prevalent in patients with vertebral deformities (53.8 %) than in those without (20 %) ($P = 0.012$). The difference in fish intake (more than twice weekly) between patients with (3.8 %) and without (20 %) vertebral deformities was marginally significant ($P = 0.073$), probably due to the small number of cases. Daily coffee or tea intake was more prevalent in patients without (34.6 %) than with (11.5 %) vertebral deformities ($P = 0.048$). The prevalence of regular menstruation was statistically different between groups ($P = 0.013$). Disease duration was longer in patients with vertebral deformities (mean 19.7 years vs. 14.5 years) ($P = 0.033$). No variables regarding BMD (spine BMD, hip BMD, spine T score, and hip T score) were associated with vertebral deformities, nor was a history of osteoporosis. A history of bone fracture was more prevalent in patients with (38.5 %) than without (11.5 %) vertebral deformities ($P = 0.025$). A history of vertebral fracture was more prevalent in patients with (21.7 %) than without (0 %) vertebral deformities ($P = 0.012$). A family history of osteoporosis or femoral neck fracture was more prevalent in patients without (96.2 %) than patients with (80.8 %) vertebral deformities ($P = 0.083$). In addition, CS use and treatment duration were associated with vertebral deformities: treatment duration was marginally longer in patients with vertebral deformities (mean 17.6 years vs 13.3 years) ($P = 0.087$). Current use of CS was more prevalent in patients without (100 %) than in patients with (84.6 %) vertebral deformities ($P = 0.037$).

Table 2 Characteristics of the systemic lupus erythematosus (SLE) patients without and with vertebral fractures were compared

Variable	All patients (<i>n</i> = 52)	SLE patients		<i>P</i> value
		Without vertebral fractures (<i>n</i> = 26)	With vertebral fractures (<i>n</i> = 26)	
Basic and lifestyle data				
Age, mean (SD)	45.2 (13.8)	40.3 (10.7)	50.0 (15.0)	0.01
BMI, mean (SD)	22.1 (3.7)	21.6 (3.1)	22.5 (4.2)	0.381
Postmenopausal status, <i>n</i> (%)	19 (37.3)	5 (20.0) ¹	14 (53.8)	0.012
Ever smoking, <i>n</i> (%)	16 (30.8)	10 (38.5)	6 (23.1)	0.229
Alcohol drinking more than thrice weekly, <i>n</i> (%)	6 (12.0)	4 (15.4)	2 (8.3) ²	0.443
Exercise more than twice weekly, <i>n</i> (%)	37 (72.5)	18 (72.0) ¹	19 (73.1)	0.931
Going out everyday, <i>n</i> (%)	21 (45.7)	9 (39.1) ³	12 (52.2) ³	0.375
Daily milk intake, <i>n</i> (%)	19 (37.3)	7 (28.0) ¹	12 (46.2)	0.18
Dairy product intake more than twice weekly, <i>n</i> (%)	10 (19.2)	4 (15.4)	6 (23.1)	0.482
Fish intake more than twice weekly, <i>n</i> (%)	6 (11.8)	5 (20.0) ¹	1 (3.8)	0.073
Small fish intake more than twice weekly, <i>n</i> (%)	21 (42.0)	12 (48.0) ¹	9 (36.0) ¹	0.39
Soybean product intake more than twice weekly, <i>n</i> (%)	5 (9.6)	4 (15.4)	1 (3.8)	0.158
Daily coffee or (black) tea intake, <i>n</i> (%)	12 (23.1)	3 (11.5)	9 (34.6)	0.048
Daily green tea intake, <i>n</i> (%)	19 (36.5)	10 (38.5)	9 (34.6)	0.773
Number of deliveries, mean (SD)	0.96 (1.15)	0.72 (1.06) ¹	1.19 (1.20)	0.144
Regular menstruation, <i>n</i> (%)	28 (57.1)	18 (75.0) ²	10 (40.0) ¹	0.013
History of falls, <i>n</i> (%)	27 (57.1)	15 (68.2) ⁴	12 (48.0) ¹	0.163
Use of bed, <i>n</i> (%)	33 (66.0)	17 (65.4)	16 (66.7) ¹	0.924
History of surgery, <i>n</i> (%)	39 (75.0)	18 (69.2)	21 (80.8)	0.337
Clinical				
Disease duration [mean (SD), years]	17.1 (8.6)	14.5 (7.8) ¹	19.7 (8.8) ¹	0.033
Spine bone mass density (BMD), mean (SD)	0.90 (0.16)	0.91 (0.14)	0.88 (0.18)	0.501
Hip bone mass density (BMD), mean (SD)	0.75 (0.15)	0.77 (0.17) ⁴	0.74 (0.14) ³	0.463
Spine T score, mean (SD)	-1.02 (1.45)	-0.85 (1.24)	-1.18 (1.64)	0.412
Hip T score, mean (SD)	-1.01 (1.33)	-0.79 (1.35) ⁴	-1.22 (1.30) ³	0.278
Spine low BMD, <i>n</i> (%)	29 (55.8)	13 (50.0)	13 (50.0)	0.402
Hip low BMD, <i>n</i> (%)	23 (51.1)	9 (40.9) ⁴	14 (60.9) ³	0.181
Spine or hip low BMD, <i>n</i> (%)	35 (70.0)	15 (62.5)	20 (76.9)	0.266
Low bone-specific alkaline phosphatase (BAP), <i>n</i> (%)	1 (2.0)	1 (4.3) ³	0 (0)	0.283
High type I collagen cross-linked N-telopeptide (NTx), <i>n</i> (%)	3 (6.1)	1 (4.3) ³	2 (7.7)	0.626
Erythrocyte sedimentation rate (ESR) [mean (SD), mm/h]	22.5 (17.3)	23.6 (15.6) ⁴	21.5 (18.9) ¹	0.68
C-reactive protein (CRP) [mean (SD), mg/dl]	0.25 (0.66)	0.17 (0.18) ¹	0.32 (0.91)	0.409
SLEDAI, mean (SD)	7.2 (6.0)	8.4 (6.1)	6.0 (5.6)	0.139
25-Hydroxyvitamin D [mean (SD), pg/ml]	55.6 (19.1)	54.5 (20.3) ³	56.6 (18.3)	0.706
Creatinine clearance (CrCl) [mean (SD), ml/min]	90.8 (31.6)	95.7 (36.3) ¹	86.0 (26.1)	0.278
Urine protein [mean (SD), g/day]	0.65 (1.35)	0.80 (1.80) ⁴	0.53 (0.84)	0.487
History of photosensitivity, <i>n</i> (%)	22 (44.9)	9 (37.5) ²	13 (52.0) ¹	0.308
Use of sunscreen, <i>n</i> (%)	38 (74.5)	17 (68.0) ¹	21 (80.8)	0.296
History of renal involvement, <i>n</i> (%)	24 (52.2)	12 (57.1) ⁴	12 (48.0) ¹	0.536
History of diabetes mellitus, <i>n</i> (%)	3 (5.8)	2 (7.7)	1 (3.8)	0.552
History of hyperlipidemia, <i>n</i> (%)	24 (47.1)	11 (44.0) ¹	13 (50.0)	0.668
History of aseptic necrosis of femoral bone, <i>n</i> (%)	15 (31.3)	6 (27.3) ⁴	9 (34.6)	0.584
History of previous osteoporosis, <i>n</i> (%)	13 (26.0)	5 (19.2)	8 (33.3) ²	0.256
History of previous bone fracture, <i>n</i> (%)	13 (25.0)	3 (11.5)	10 (38.5)	0.025
History of previous vertebral fracture, <i>n</i> (%)	5 (10.2)	0 (0)	5 (21.7) ³	0.012
Family history of osteoporosis or femoral neck fracture, <i>n</i> (%)	46 (88.5)	25 (96.2)	21 (80.8)	0.083